AGU PUBLICATIONS

JGR

Journal of Geophysical Research: Atmospheres

RESEARCH ARTICLE

10.1002/2016JD026315

Special Section:
Quantifying the emission, properties, and diverse impacts of wildfire smoke

Key Points:
- Emission factors (EFs) were measured for three western wildfires for major gases and particles and rarely measured OVOCs and organic nitrates
- Aircraft-measured EF(PM_1) from wildfires is more than 2 times that of prescribed fires
- Emission estimates for western U.S. wildfires indicate a significant BB contribution to aerosol mass

Supporting Information:
- Supporting Information S1

Correspondence to:
L. G. Huey,
greg.huey@eas.gatech.edu

Citation:
Liu, X., et al. (2017), Airborne measurements of western U.S. wildfire emissions: Comparison with prescribed burning and air quality implications, *J. Geophys. Res. Atmos.*, *122*, doi:10.1002/2016JD026315.

Received 6 DEC 2016
Accepted 20 APR 2017

Airborne measurements of western U.S. wildfire emissions: Comparison with prescribed burning and air quality implications

Xiaoxi Liu[1,2,3], L. Gregory Huey[1], Robert J. Yokelson[4], Vanessa Selimovic[4], Isobel J. Simpson[5], Markus Müller[4,6], Jose L. Jimenez[7,8], Pedro Campuzano-Jost[7,8], Andreas J. Beyersdorf[9,10], Donald R. Blake[5], Zachary Butterfield[11,12], Yonghoon Choi[9,13], John D. Crounse[14], Douglas A. Day[7,8], Glenn S. Diskin[9], Manvendra K. Dubey[11], Edward Fortner[15], Thomas F. Hanisco[16], Weiwei Hu[7,8], Laura E. King[1], Lawrence Kleinman[17], Simone Meinardi[5], Tomas Mikoviny[18], Timothy B. Onasch[15], Brett B. Palm[7,8], Jeff Peischl[7,19], Ilana B. Pollack[7,19,20], Thomas B. Ryerson[19], Glen W. Sachse[9], Arthur J. Sedlacek[17], John E. Shilling[21], Stephen Springston[17], Jason M. St. Clair[14,22,23], David J. Tanner[1], Alexander P. Teng[14], Paul O. Wennberg[14,24], Armin Wisthaler[6,18], and Glenn M. Wolfe[16,25]

[1]School of Earth and Atmospheric Sciences, Georgia Institute of Technology, Atlanta, Georgia, USA, [2]Now at Cooperative Institute for Research in Environmental Sciences, University of Colorado Boulder, Boulder, Colorado, USA, [3]Now at Department of Chemistry, University of Colorado Boulder, Boulder, Colorado, USA, [4]Department of Chemistry, University of Montana, Missoula, Montana, USA, [5]Department of Chemistry, University of California, Irvine, California, USA, [6]Institute for Ion Physics and Applied Physics, University of Innsbruck, Innsbruck, Austria, [7]Cooperative Institute for Research in Environmental Sciences, University of Colorado Boulder, Boulder, Colorado, USA, [8]Department of Chemistry, University of Colorado Boulder, Boulder, Colorado, USA, [9]NASA Langley Research Center, Hampton, Virginia, USA, [10]Now at Department of Chemistry, California State University, San Bernardino, California, USA, [11]Earth and Environmental Sciences Division, Los Alamos National Laboratory, Los Alamos, New Mexico, USA, [12]Now at Department of Atmospheric, Oceanic, and Space Sciences, University of Michigan, Ann Arbor, Michigan, USA, [13]Science Systems and Applications, Inc., Hampton, Virginia, USA, [14]Division of Geological and Planetary Sciences, California Institute of Technology, Pasadena, California, USA, [15]Center for Aerosol and Cloud Chemistry, Aerodyne Research Inc., Billerica, Massachusetts, USA, [16]Atmospheric Chemistry and Dynamics Laboratory, NASA Goddard Space Flight Center, Greenbelt, Maryland, USA, [17]Environmental and Climate Sciences Department, Brookhaven National Laboratory, Upton, New York, USA, [18]Department of Chemistry, University of Oslo, Oslo, Norway, [19]Earth System Research Laboratory, National Oceanic and Atmospheric Administration, Boulder, Colorado, USA, [20]Now at Department of Atmospheric Science, Colorado State University, Fort Collins, Colorado, USA, [21]Atmospheric Sciences and Global Change Division, Pacific Northwest National Laboratory, Richland, Washington, USA, [22]Now at Atmospheric Chemistry and Dynamics Laboratory, NASA Goddard Space Flight Center, Greenbelt, Maryland, USA, [23]Now at Joint Center for Earth Systems Technology, University of Maryland, Baltimore County, Baltimore, Maryland, USA, [24]Division of Engineering and Applied Science, California Institute of Technology, Pasadena, California, USA, [25]Joint Center for Earth Systems Technology, University of Maryland, Baltimore County, Baltimore, Maryland, USA

Abstract Wildfires emit significant amounts of pollutants that degrade air quality. Plumes from three wildfires in the western U.S. were measured from aircraft during the Studies of Emissions and Atmospheric Composition, Clouds and Climate Coupling by Regional Surveys (SEAC^{4}RS) and the Biomass Burning Observation Project (BBOP), both in summer 2013. This study reports an extensive set of emission factors (EFs) for over 80 gases and 5 components of submicron particulate matter (PM_1) from these temperate wildfires. These include rarely, or never before, measured oxygenated volatile organic compounds and multifunctional organic nitrates. The observed EFs are compared with previous measurements of temperate wildfires, boreal forest fires, and temperate prescribed fires. The wildfires emitted high amounts of PM_1 (with organic aerosol (OA) dominating the mass) with an average EF that is more than 2 times the EFs for prescribed fires. The measured EFs were used to estimate the annual wildfire emissions of carbon monoxide, nitrogen oxides, total nonmethane organic compounds, and PM_1 from 11 western U.S. states. The estimated gas emissions are generally comparable with the 2011 National Emissions Inventory (NEI). However, our PM_1 emission estimate (1530 ± 570 Gg yr^{-1}) is over 3 times that of the NEI $PM_{2.5}$ estimate and is also higher than the $PM_{2.5}$ emitted from all other sources in these states in the NEI. This study indicates that the source of OA from biomass burning in the western states is significantly underestimated. In addition, our results indicate that prescribed burning may be an effective method to reduce fine particle emissions.

Plain Language Summary Wildfires emit large amounts of pollutants. This work quantifies the emissions of a range of both gaseous and particulate species from U.S. wildfires using measurements performed on research aircraft. The results indicate that wildfires are a large source of particulate pollution in the western states and that the source is currently underestimated by more than a factor of three in emissions inventories. Comparison of these results to those obtained from prescribed burning indicates that wildfires are a larger source of pollution.

1. Introduction

Open biomass burning (BB), including wildfires and prescribed agricultural and forest management burns, is a large global source of trace gases and aerosol [*Crutzen and Andreae*, 1990]. In the U.S., wildfires are the largest contributor to the annual total area burned and occur largely in the western continental states and Alaska (National Interagency Coordination Center, https://www.nifc.gov/fireInfo/fireInfo_statistics.html). While wildfires perform many beneficial ecosystem functions [*Kilgore*, 1981], they also degrade U.S. air quality [*Park et al*., 2007; *Jaffe et al*., 2008; *Singh et al*., 2012; *Brey and Fischer*, 2016]. For example, summer wildfires produce a substantial fraction of the fine aerosol mass in the contiguous U.S., and their interannual variability dominates the fluctuations of carbonaceous aerosol concentrations [*Park et al*., 2007]. In the 2011 National Emissions Inventory (NEI), open fires accounted for 37% of fine particulate matter ($PM_{2.5}$) emitted in the U.S., with wildfires contributing more than half of that total. In addition, wildfires release substantial amounts of gaseous pollutants including ozone precursors [*Andreae and Merlet*, 2001; *Akagi et al*., 2011]. Ozone (O_3) production is common from wildfires in tropical and temperate regions, while both O_3 production and destruction have been observed in boreal wildfire plumes [*Goode et al*., 2000; *Hobbs et al*., 2003; *Alvarado et al*., 2010; *Singh et al*., 2010; *Jaffe and Wigder*, 2012]. PM, O_3, and many other primary emissions and secondary products have negative health effects, which can be exacerbated when the smoke impacts populated areas [*Künzli et al*., 2006; *Naeher et al*., 2007; *Delfino et al*., 2009]. A possible mechanism for PM's adverse health effect is a particle's ability to generate reactive oxygen species, referred to as oxidative potential [*Donaldson et al*., 2005]. Recent studies based on dithiothreitol assay measurements find that BB plays a large role in $PM_{2.5}$ oxidative potential, which is strongly associated with respiratory and cardiovascular diseases in epidemiological studies [*Verma et al*., 2014; *Fang et al*., 2016; *Yang et al*., 2016]. This further points to the potential of BB $PM_{2.5}$ for adverse health effects.

Prescribed burning is a commonly used land management practice implemented under specified fuel, meteorological, and dispersion conditions. It maintains the beneficial role of fire while minimizing smoke impacts, consuming accumulated fuels that could otherwise be conducive to wildfires, thus reducing wildfire hazards [*Biswell*, 1999; *Hardy et al*., 2001]. Currently, the understanding of the tradeoffs between the use of prescribed fires versus wildfires is limited, as it requires an understanding of fires and their emissions, climate change, and human activity [*Marlon et al*., 2012]. Climate change has contributed to increases in wildfire size and frequency and to the length of the fire season in the western U.S. [*Westerling et al*., 2006]. Other human activities, including land use change and wildfire management strategies such as suppression, prevention, and fuel treatments, impact wildfire frequency and intensity as well [*Savage and Swetnam*, 1990; *Belsky and Blumenthal*, 1997; *Stevens et al*., 2014]. In addition, a detailed knowledge of the emissions and smoke chemistry of wildfires and prescribed burning is crucial to understand potential advantages of prescribed burns relative to wildfires. For example, wildfires typically consume more fuel per unit area than prescribed fires [*Campbell et al*., 2007; *Turetsky et al*., 2011; *Yokelson et al*., 2013]. Higher fuel consumption coupled with potentially different emission factors (EFs) [*Urbanski*, 2013] suggests that prescribed fires and wildfires may have different total emissions and regional smoke impacts. Prescribed forest fire emissions were measured extensively between 2009 and 2013 across the U.S. temperate ecosystems in a series of studies [*Burling et al*., 2011; *Akagi et al*., 2013; *Yokelson et al*., 2013; *May et al*., 2014; *Müller et al*., 2016]. However, the information available on wildfire emissions in temperate forests of the contiguous U.S. is limited to a few fires sampled from Oregon and Idaho in the 1980s, Montana in the 1990s, and from the northern Rocky Mountains recently [*Radke et al*., 1991; *Friedli et al*., 2001; *Urbanski*, 2013]. The goal of this study is to provide information about primary emissions from western U.S. wildfires to inform future fire management and atmospheric chemistry studies.

In the summer of 2013, two field campaigns sampled multiple wildfires in the western U.S. The Biomass Burning Observation Project (BBOP) deployed the Department of Energy (DOE) Gulfstream-1 (G-1) aircraft to study wildfires and agricultural burns and how the impacts of their emissions evolve with time. The G-1

aircraft was equipped with a suite of instruments for measuring aerosol, trace gases, and atmospheric state parameters. Emissions from 17 wildfires in the western continental U.S. and over 24 agricultural burns in the southeastern U.S. were sampled from July to October 2013. Meanwhile, from August to September 2013, the Studies of Emissions and Atmospheric Composition, Clouds and Climate Coupling by Regional Surveys (SEAC^{4}RS) airborne field campaign intercepted plumes from 15 agricultural and over 10 forest fires in the western, central, and southeastern U.S. The heavily instrumented NASA DC-8 research aircraft was deployed during this mission, which enabled measurements of a wide variety of chemical species and physical parameters [*Forrister et al*., 2015; *Liu et al*., 2016; *Toon et al*., 2016]. Here we focus on the initial emissions from the three wildfires where freshly emitted plumes were intercepted by the aircraft: the Colockum Tarps fire sampled during BBOP and the Big Windy Complex and the Rim Fire sampled during SEAC^{4}RS. We also compare emissions from the three studied wildfires with those from other temperate and boreal wildfires and some prescribed fires obtained from aircraft. With the calculated EFs, we estimate the annual wildfire emissions of carbon monoxide (CO), nitrogen oxides (NO_x), nonmethane organic compounds (NMOCs), and submicron particulate matter (PM_1) in the western U.S.

2. Methods

2.1. Platforms and Instrumentation

In situ measurements were conducted from the DOE G-1 aircraft during BBOP and the NASA DC-8 aircraft during SEAC^{4}RS. Table 1 summarizes the BBOP trace gas and particle measurements used in this work, along with methodologies, sample intervals, accuracies, and references. The set of SEAC^{4}RS measurements used to characterize wildfire emissions were almost identical to that used for agricultural fires in the southeastern U.S., which can be found in *Liu et al*. [2016], with the addition of a set of volatile organic compounds (VOCs) measured by whole air sampling (WAS) [*Simpson et al*., 2011] and several oxygenated volatile organic compounds (OVOCs) and organic nitrates measured by chemical ionization mass spectrometry (CIMS) [*Crounse et al*., 2006; *Paulot et al*., 2009a; *St. Clair et al*., 2014; *Teng et al*., 2015]. All aircraft data used were synchronized to a common time scale with 1 Hz resolution.

While full details of most instruments deployed for BBOP are available in the references cited in Table 1, here we describe a few exceptions. CO was measured on the G-1 by a commercial instrument based on cavity enhanced absorption (Los Gatos Research, San Jose, CA). O_3 was measured by a commercial analyzer (Thermo Scientific Model 49i) that was modified for internal calibrations. A commercial SO_2 analyzer (Thermo Scientific 43i) was modified to provide an internal chemical zero. The $NO/NO_2/NO_y$ instrument was custom built by Air Quality Design, Inc. (Golden, CO). It was calibrated both on the ground and in flight by a standard addition of a known amount of NO. The instrumental conversion efficiency of NO_2 to NO was determined before each flight. Zero air was sampled periodically during flight to determine artifact signals, which were then subtracted from ambient signals during data reduction. More details on the methods and accuracies are listed in Table 1.

2.2. Fire Descriptions

Table 2 summarizes the locations, sizes, fuels, and local time of fresh plume intercepts of the three wildfires. Figure 1 shows the flight tracks near the fires, color-coded by measured CO concentrations. The Colockum Tarps fire started in the vicinity of Malaga, WA, on 27 July 2013 and grew from 14,000 ha to 24,000 ha 3 days later on the day when its smoke was sampled. Fuels burned were mainly timber, grass, and brush. The G-1 aircraft sampled fresh and downwind plumes in both the morning and afternoon on 30 July 2013 southeast of Wenatchee, WA. The four fresh plumes used for this analysis, less than ~20 min old, were obtained near the source at 1.2 to 1.3 km above the ground. The Big Windy Complex started on 26 July 2013 and consisted of three large fires, which burned approximately 40 km northwest of Grants Pass, OR. On the day of sampling (6 August 2013), the Big Windy Complex grew from 668 ha to 4389 ha, burning timber and brush. Fresh plumes were intercepted by the NASA DC-8 aircraft at altitudes ranging from 1.5 to 2.3 km above the ground. The Rim Fire started on 17 August 2013 in the Stanislaus National Forest, about 3 km northeast of Buck Meadows, CA. On the day of sampling (26 August 2013), the fire was in its intense, primary burning period and burned more than 8000 ha in 1 day [*Peterson et al*., 2014; *Yates et al*., 2016]. The Rim Fire fuel types included timber, brush, and chaparral. Fresh samples were obtained at ~2.6 km above the ground. For the two SEAC^{4}RS fires, the DC-8 sampled smoke that extended tens of kilometers during plume penetrations up to 6 min in duration

Table 1. G-1 Aircraft Measurements Used in This Work

Measurement	Method	Sample Interval	Calibration Accuracy	Reference/Instrument
CO_2 and CH_4	Cavity ring down spectroscopy	~1 s	<70 ppb for CO_2, <0.5 ppb for CH_4	*Crosson* [2008]/Picarro Inc.
CO	Cavity enhanced absorption	1 s	2%	Los Gatos Research
NO, NO_2, and NO_y	Chemiluminescence	1 s	10%	Air Quality Design, Inc.
VOCs and OVOCs	Proton transfer reaction mass spectrometry	0.1 s @ ~3.4 s[a]	5–15%	*Lindinger et al.* [1998] and *Shilling et al.* [2013]
SO_2	Pulsed fluorescence	1 s	~5–10%	Thermo Scientific 43i
O_3	UV optical absorption	1 s	5%	Thermo Scientific 49i
Nonrefractory submicron aerosol (sulfate, nitrate, ammonium, chloride, and organics)[b]	Soot particle aerosol mass spectrometry	1 s	38%	*Bahreini et al.* [2009]

[a]Disjunct sampling.
[b]Particle diameter less than 1 μm. A collection efficiency of 0.5 was used, though this may overestimate the nonrefractory PM for dual vaporizer modes (refer to *Onasch et al.* [2012, Table 1] and discussions in *Lee et al.* [2015]).

(Table 2). The Big Windy Complex plumes used for analysis were estimated to have aged ~1 h after emission according to wind speeds measured aboard aircraft and the locations of burning spots detected from Moderate Resolution Imaging Spectroradiometer (MODIS). The Rim Fire samples included near-source plume penetrations. The age of the relatively fresh Rim Fire samples smoke ranged from ~20 min to ~2 h as distance from source increased. Figure S2 in the supporting information shows examples of time series obtained from the three fires.

2.3. Calculation of Emission Ratios, Emission Factors, and Modified Combustion Efficiency

This work considers only fresh smoke samples as described above. For each fresh plume intercept, the average excess mixing ratio of a species X (ΔX) was calculated by subtracting the average mixing ratio of X in the background air from that in the fire plume. The background samples were taken just outside the plume at a similar location and altitude. We computed molar emission ratios (ERs) for gaseous species and mass ERs for particulate species for each fire as follows. During the two BBOP flights on 30 July 2013, four fresh, thick plumes from the Colockum Tarps fire with similar enhancement magnitudes were intercepted. To allow comparison between measurements with different time resolution and response times, we calculated plume-averaged ERs by dividing the integral of ΔX by the integral of simultaneously measured ΔCO_2. Here the integrals were calculated by summing ΔX values spanning the duration of discrete samples listed in Table 2. The four plume-averaged ERs were subsequently used to calculate four plume-averaged EFs. The fire average was calculated from the four plume samples. The fresh plume samples obtained for the Big Windy Complex and the Rim Fire during SEAC[4]RS consisted of both thick and thin plumes. To better weight larger excess mixing ratios that have higher signal-to-noise ratios, fire-averaged ERs for SEAC[4]RS fires were determined from the slope of the linear least squares line of a plot of the integral of ΔX versus that of ΔCO_2 (or ΔCO) for each fire with the intercept forced to 0 [*Yokelson et al.*, 1999]. This method works well for relatively fast measurements with time resolution ≤3 s, since the plume edges can be well defined. However, species measured by the WAS system were treated differently, since they were collected over a 0.5–1 min period

Table 2. Details of the Wildfires Sampled in the Western U.S.

Date	Fire Name	Latitude	Longitude	Final Area Burned (ha)	Location	Fuel Description	Fresh Plume Local Time
30 July 2013	Colockum Tarps	47.30	−120.11	32,463	Malaga, WA	Timber (mixed conifer), grass, and brush	09:31–09:32, 10:33–10:35, 13:17–13:19, and 14:08–14:09
6 August 2013	Big Windy Complex	42.63	−123.86	10,435	Grants Pass, OR	Timber (mixed conifer and oak) and brush	15:53–15:55, 16:17–16:20, 16:21–16:24, and 16:32–16:38
26 August 2013	Rim Fire	37.86	−120.09	104,176	Buck Meadows, CA	Timber (mixed conifer and oak), brush, and chaparral	15:59–16:01, 16:03–16:07, and 16:13–16:19

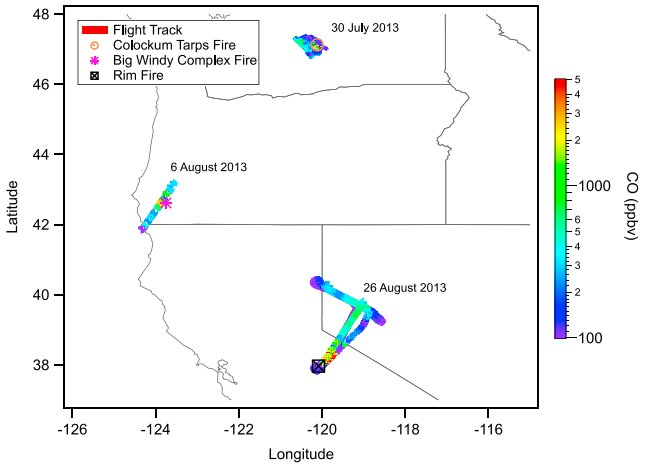

Figure 1. Map of the three wildfires and flight tracks near the fire sources during BBOP and SEAC^{4}RS. Flight tracks are colored by measured CO concentrations. The dates indicate the day each fire was sampled.

every 1–2 min during plume encounters. A total of 8 and 11 WAS samples were collected for the Big Windy Complex and the Rim Fire, respectively. The fire-averaged ERs of WAS species were determined as the slope (with the intercept forced to 0) of a plot of available discrete WAS ΔX versus WAS ΔCO. The fire-averaged ERs of the Big Windy Complex and the Rim Fire were then used for fire-averaged EF calculations. If we use the slope-based method to derive fire-averaged EFs for the Colockum Tarps fire, the difference is less than 10% compared to the plume-averaged method. The small difference was expected since the plumes of the Colockum Tarps fire were of similar sizes so the slope-based method weighted each plume similarly.

A set of ERs can be used to calculate a set of EFs, in units of grams of compound X emitted per kilogram of dry biomass burned. For the Colockum Tarps fire, we used its plume-averaged ERs to calculate a set of plume-averaged EFs and then derive the fire-averaged EFs by averaging the plume-averaged EFs. The fire-averaged EFs for the other two fires were derived using the single fire-averaged ERs. All EF calculations were based on the carbon mass balance method assuming that all of the volatilized carbon was detected [*Yokelson et al*., 1999; *Liu et al*., 2016]. The carbon mass fraction of consumed fuel was set as 45.7% [*Santín et al*., 2015]. In a departure from previous studies that generally assume a fraction of 50% based on fuel elemental analysis [*Susott et al*., 1996; *Burling et al*., 2010], *Santín et al*. [2015] directly quantified C emitted to the atmosphere by a boreal forest fire. Since charcoal production may be significant for wildfires, using the percentage of carbon in the volatilized fuel is a preferred implementation of the carbon mass balance calculation when charcoal production is significant as discussed elsewhere [*Bertschi et al*., 2003b]. Note that EFs scale linearly with the assumed carbon mass fraction. The sum of the emitted carbon was determined from the sum of measured gaseous and particulate carbon-containing compounds. This sum could underestimate the total carbon by 1–2% due to unmeasured carbon, which would lead to an overestimation of EFs by 1–2% [*Akagi et al*., 2011], which is small compared to the variability and uncertainty of these EFs. Although fewer VOC species were measured during BBOP, the overestimation of EFs using this method would not exceed 4% since CO_2, CO, and methane (CH_4) often account for over ~96% of the total emitted carbon [*Akagi et al*., 2011]. For the two SEAC^{4}RS fires, we report the errors of individual EFs as combined uncertainties that vary by species and by fire and that could be quantified here, including (1) the uncertainties in the integrated ΔX, which are assumed to be instrumental uncertainties given the significant enhancements in fresh plumes and (2) the uncertainties in the slopes of ΔX versus ΔCO_2 (or ΔCO), which are usually $<$10%. For the Colockum Tarps fire, we used the standard deviations of the four plume-averaged EFs to represent EF uncertainties, which are generally larger than the combined instrumental and slope uncertainties.

BB emissions also vary with flaming and smoldering combustion processes. Modified combustion efficiency (MCE), defined as $\Delta CO_2/(\Delta CO_2 + \Delta CO)$, was calculated to describe the relative amount of flaming or smoldering [*Akagi et al*., 2011]. MCE can range over a large range, from $<$0.8 for smoldering combustion to 0.99 for flaming combustion. An MCE near 0.9 suggests roughly equal amounts of flaming and smoldering [*Akagi et al*., 2011].

3. Results and Discussion

We use the airborne measurements to determine the composition of the emissions generated during major fire events, which could then lead to widespread air quality impacts via long-range transport. However, these

airborne measurements did not capture smoke that was produced by residual smoldering combustion (RSC), during which smoke was not lofted by flame-induced convection [*Bertschi et al*., 2003a]. The RSC emissions often contribute more to local (near-fire) impacts, but they also impact the total emissions over the lifetime of the fire. In general, RSC would most often increase the whole fire EF for smoldering dominated species. Thus, the EFs for smoldering dominated species measured in this work may underestimate the total emissions from these fires. Another factor that potentially influences the EFs of some very reactive species (such as monoterpenes and NO_x) reported in this work is photochemical processing. Although only relatively fresh (<20 min to ~120 min) samples were used, elevated O_3 (maximum ΔO_3 of 100 ppbv in the Rim Fire plumes) was observed for all three fires and elevated peroxyacetyl nitrate (PAN) up to ~9.4 ppbv was observed for the two SEAC^{4}RS fires where PAN measurements were available. Both O_3 and PAN formation indicated rapid photochemical processing. The observed $\Delta O_3/\Delta CO$ ratios in these plumes were approximately 0.01. Similar ERs of $\Delta O_3/\Delta CO$ have also been observed in prescribed forest and agricultural fire plumes less than ~20 min old [*Akagi et al*., 2013; *Liu et al*., 2016].

Table 3 shows the average EFs and MCEs for the three wildfires along with the study-averaged EFs and MCE. Among the chemical species that were quantified from the NASA DC-8 platform, we identified over 80 trace gases and 5 fine particle components that were significantly elevated within the wildfire plumes when compared with their background levels. Meanwhile, emissions of 14 gases and 5 fine particle components were acquired from the G-1 aircraft. This represents the most comprehensive suite of species measured in the field for U.S. wildfires to date. The fire-integrated MCEs derived in this work range from 0.877 to 0.935, corresponding to ~41%–71% nominal flaming fractions.

3.1. Initial Emissions of Trace Gases

For the Big Windy Complex and the Rim Fire, the emitted gases include carbon dioxide (CO_2); CO; CH_4; hydrogen peroxide (H_2O_2); sulfur species; hydrochloric acid (HCl); six halocarbons; nitrogen-containing compounds; all the measured alkanes, alkenes, alkynes, and aromatics; and a variety of OVOCs. Benzene and toluene were measured by both WAS and a proton-transfer-reaction mass spectrometer (PTR-MS). Good agreement was found between WAS and PTR-MS measurements of benzene (EFs within 8%) and toluene (EFs within 24%). We reported EFs of benzene and toluene as the averages of the two techniques. The gases that were measured, but deemed not to be emitted by the fires, were primarily halocarbons that were either not enhanced or had weak correlations with CO ($r^2 < 0.6$). A list of these gases can be found in Table 4 of *Simpson et al*. [2011] with a few exceptions discussed in section 3.1.2. *Yates et al*. [2016] has also reported some Rim Fire EFs as measured on 26 August 2013 from the DC-8 aircraft, namely, CO_2, CO, CH_4, methanol, acetonitrile (CH_3CN), acetone/propanal, benzene, and toluene. Despite potential differences in fresh plume selection and different assumptions made for the carbon mass balance method, our Rim Fire EFs agree with those of *Yates et al*. [2016] to within the stated uncertainties. For the Colockum Tarps fire, the emissions of 14 gases were measured: CO_2, CO, CH_4, sulfur dioxide (SO_2), NO_x, two aromatics (benzene and toluene), CH_3CN, and five OVOCs.

Study-averaged EFs were calculated from the EFs of all three fires if available or the two SEAC^{4}RS fires if the species was not measured during BBOP. The three exceptions are carbonyl sulfide that was only emitted from the Rim Fire, *n*-heptane only emitted from the Big Windy Complex, and 2,3-butanedione only measured from the Colockum Tarps fire during BBOP. The uncertainties reported for the study averages are the standard deviations of the EFs for single fires and thus represent fire-to-fire variability. Note that for a few species that were measured with measurement uncertainties of 30–50%, such as hydrogen cyanide (HCN), the fire-to-fire variability is smaller than the single-fire uncertainty (Table 3).

According to the study-averaged EFs, the major gaseous emissions by mass are (EF > 0.5 g kg^{-1}; Table 3 and Figure 2): CO_2 (1454 ± 78), CO (89.3 ± 28.5), CH_4 (4.90 ± 1.50), methanol (2.45 ± 1.43), formaldehyde (2.29 ± 0.27), 2,3-butanedione (2.10 ± 0.63), acetaldehyde (1.64 ± 0.52), acetone/propanal (1.13 ± 0.82), hydroxyacetone (1.13 ± 0.31), ethene (0.91 ± 0.17), ethane (0.72 ± 0.25), H_2O_2 (0.60 ± 0.60), NO_2 (0.58 ± 0.50), and furan (0.51 ± 0.06). Also listed in Table 3 are average gaseous EFs from previous airborne studies of forest fires: boreal forest fires over Canada [*Simpson et al*., 2011], seven prescribed fires burning pine-forest understory in longleaf pine stands in South Carolina [*Akagi et al*., 2013], and a compilation by *Akagi et al*. [2011] of temperate evergreen forest fires (which included only two confirmed wildfires) in North America. Detailed

Table 3. Measured MCEs and Emission Factors (g kg^{-1}) for the Three Wildfires in the Western U.S. and Comparison With Aircraft-Measured EFs From Previous Forest Fire Studies[a]

Fire		Colockum Tarps	Big Windy Complex	Rim Fire	Study Average	Temperate Forests	Prescribed Fires in South Carolina	Boreal Forests
Reference		This Work	This Work	This Work	This Work	*Akagi et al.* [2011]	*Akagi et al.* [2013]	*Simpson et al.* [2011]
MCE		0.935	0.877	0.923	0.912	0.92	0.931	0.89
Compound	Formula							
Carbon dioxide	CO_2	1517 (20)	1367 (47)	1478 (11)	1454 (78)	1637 (71)	1675 (42)	1616 (180)
Carbon monoxide	CO	67.6 (12.7)	122 (8)	78.7 (4.0)	89.3 (28.5)	89 (32)	79 (19)	113 (72)
Methane	CH_4	3.70 (0.31)	6.59 (0.35)	4.43 (0.25)	4.90 (1.50)	3.92 (2.39)	2.66 (1.77)	4.7 (2.9)
Hydrogen peroxide	H_2O_2	–	1.02 (0.35)	0.18 (0.06)	0.60 (0.60)	–	–	–
Sulfur dioxide	SO_2	0.75 (0.06)	0.11 (0.02)	0.11 (0.02)	0.32 (0.37)	2.03 (1.79)	–	–
Carbonyl sulfide	OCS	–	–	$5.9\ (0.9) \times 10^{-3}$	$5.9\ (0.9) \times 10^{-3}$	–	0.01 (0.003)	0.029 (0.007)
Dimethyl sulfide	C_2H_6S	–	$5.7\ (1.2) \times 10^{-3}$	$5.6\ (1.2) \times 10^{-4}$	$3.1\ (3.6) \times 10^{-3}$	–	0.008 (0.003)	$2.3\ (1.2) \times 10^{-3}$
Hydrochloric acid	HCl	–	$3.2\ (1.1) \times 10^{-3}$	$4.6\ (1.2) \times 10^{-3}$	$3.9\ (1.0) \times 10^{-3}$	–	–	–
Methyl chloride	CH_3Cl	–	0.038 (0.005)	0.017 (0.002)	0.027 (0.015)	–	–	0.029 (0.007)
Dichloromethane	CH_2Cl_2	–	$1.9\ (0.3) \times 10^{-3}$	$6.5\ (1.8) \times 10^{-4}$	$1.3\ (0.9) \times 10^{-3}$	–	–	–
1,2-Dichloroethane	$C_2H_4Cl_2$	–	$1.1\ (0.2) \times 10^{-3}$	$5.1\ (1.3) \times 10^{-4}$	$8.2\ (4.4) \times 10^{-4}$	–	–	$6.4\ (5.1) \times 10^{-4}$
Methyl iodide	CH_3I	–	$5.5\ (1.2) \times 10^{-4}$	$1.9\ (0.4) \times 10^{-4}$	$3.7\ (2.6) \times 10^{-4}$	–	–	$3.9\ (0.9) \times 10^{-4}$
Methyl bromide	CH_3Br	–	$1.3\ (0.2) \times 10^{-3}$	$2.9\ (0.4) \times 10^{-4}$	$8.1\ (7.3) \times 10^{-4}$	–	–	$1.8\ (0.5) \times 10^{-3}$
Dibromomethane	CH_2Br_2	–	$2.0\ (0.5) \times 10^{-4}$	$1.6\ (0.3) \times 10^{-4}$	$1.8\ (0.3) \times 10^{-4}$	–	–	$4.1\ (8.0) \times 10^{-5}$
HCFC-141b[b]	$C_2H_3Cl_2F$	–	$1.4\ (0.2) \times 10^{-3}$	$5.1\ (1.1) \times 10^{-4}$	$9.7\ (6.5) \times 10^{-4}$	–	–	–
HCFC-142b[b]	$C_2H_2ClF_2$	–	$3.9\ (1.2) \times 10^{-4}$	$1.3\ (0.3) \times 10^{-4}$	$2.6\ (1.8) \times 10^{-4}$	–	–	–
HFC-152a[b]	$C_2H_4F_2$	–	$1.1\ (0.2) \times 10^{-3}$	$2.4\ (1.1) \times 10^{-4}$	$6.8\ (6.2) \times 10^{-4}$	–	–	–
Nitrogen monoxide	NO	0.23 (0.04)	$8.0\ (1.4) \times 10^{-3}$	0.094 (0.018)	0.11 (0.11)	–	0.32 (0.07)	–
Nitrogen dioxide	NO_2	1.1 (0.4)	0.091 (0.011)	0.56 (0.09)	0.58 (0.50)	–	1.72 (0.32)	–
NO_x as NO	NO_x	0.94 (0.29)	0.067 (0.008)[c]	0.46 (0.08)	0.49 (0.44)	2.51 (1.02)	1.31 (0.23)	–
Hydrogen cyanide	HCN	–	0.43 (0.22)	0.25 (0.13)	0.34 (0.12)	0.73 (0.19)	0.66 (0.27)	0.89 (0.29)
Acetonitrile	CH_3CN	0.39 (0.14)	0.23 (0.05)	0.13 (0.02)	0.25 (0.13)	–	–	0.3 (0.06)
Ethanal nitrate	$C_2O_4H_3N$	–	$2.6\ (1.3) \times 10^{-3}$	$2.9\ (1.5) \times 10^{-3}$	$2.7\ (0.3) \times 10^{-3}$	–	–	–
Ethene hydroxynitrate	$C_2O_4H_5N$	–	0.018 (0.010)	$8.5\ (4.3) \times 10^{-3}$	0.013 (0.007)	–	–	–
Propanone nitrate	$C_3O_3H_5N$	–	$4.5\ (2.5) \times 10^{-3}$	$3.5\ (1.8) \times 10^{-3}$	$4.0\ (0.7) \times 10^{-3}$	–	–	–
Propene hydroxynitrates	$C_3O_4H_7N$	–	0.027 (0.008)	0.015 (0.005)	0.021 (0.008)	–	–	–
Butadiene hydroxynitrates	$C_4O_4H_7N$	–	0.017 (0.008)	0.012 (0.006)	0.014 (0.003)	–	–	–
Butene hydroxynitrates	$C_4O_4H_9N$	–	0.034 (0.017)	0.024 (0.012)	0.029 (0.007)	–	–	–
Methyl vinyl ketone/ methacrolein hydroxynitrates	$C_4O_5H_7N$	–	0.024 (0.008)	0.017 (0.005)	0.021 (0.005)	–	–	–
Isoprene hydroxynitrates	$C_5O_4H_9N$	–	0.021 (0.007)	0.013 (0.004)	0.017 (0.006)	–	–	–
Nitroxyhydroperoxide/ nitroxyhydroxyepoxide	$C_5O_5H_9N$	–	0.017 (0.009)	0.020 (0.010)	0.019 (0.002)	–	–	–
Methyl nitrate	CH_3NO_3	–	$1.7\ (0.2) \times 10^{-3}$	$1.3\ (0.2) \times 10^{-3}$	$1.5\ (0.4) \times 10^{-3}$	–	–	$1.4\ (0.9) \times 10^{-3}$
Ethyl nitrate	$C_2H_5NO_3$	–	$1.3\ (0.2) \times 10^{-3}$	$3.5\ (0.5) \times 10^{-4}$	$8.4\ (6.9) \times 10^{-4}$	–	–	$8.8\ (4.5) \times 10^{-4}$
i-Propyl nitrate	$C_3H_7NO_3$	–	$3.3\ (0.5) \times 10^{-3}$	$5.8\ (0.8) \times 10^{-4}$	$2.0\ (2.0) \times 10^{-3}$	–	–	$1.6\ (1.0) \times 10^{-3}$
n-Propyl nitrate	$C_3H_7NO_3$	–	$7.3\ (1.1) \times 10^{-4}$	$1.6\ (0.2) \times 10^{-4}$	$4.4\ (4.0) \times 10^{-4}$	–	–	$1.6\ (1.2) \times 10^{-4}$
2-Butyl nitrate	$C_4H_9NO_3$	–	$1.9\ (0.3) \times 10^{-3}$	$2.6\ (0.4) \times 10^{-4}$	$1.1\ (1.1) \times 10^{-3}$	–	–	$1.9\ (1.2) \times 10^{-3}$
3-Methyl-2-butyl nitrate	$C_5H_{11}NO_3$	–	$6.7\ (1.2) \times 10^{-4}$	$1.1\ (0.1) \times 10^{-4}$	$3.9\ (4.0) \times 10^{-4}$	–	–	$5.7\ (4.6) \times 10^{-4}$
3-Pentyl nitrate	$C_5H_{11}NO_3$	–	$4.4\ (0.7) \times 10^{-4}$	$4.4\ (1.0) \times 10^{-5}$	$2.4\ (2.8) \times 10^{-4}$	–	–	$2.6\ (1.7) \times 10^{-4}$
2-Pentyl nitrate	$C_5H_{11}NO_3$	–	$5.2\ (0.9) \times 10^{-4}$	$5.1\ (0.8) \times 10^{-5}$	$2.8\ (3.3) \times 10^{-4}$	–	–	$4.8\ (3.1) \times 10^{-4}$
Methanol	CH_3OH	1.81 (0.44)	4.09 (0.93)	1.44 (0.22)	2.45 (1.43)	1.93 (1.38)	1.20 (0.49)	1.2 (0.3)
Formaldehyde	HCHO	–	2.49 (0.26)	2.10 (0.21)	2.29 (0.27)	2.27 (1.13)	1.87 (0.27)	–
Acetaldehyde	C_2H_4O	1.64 (0.27)	2.16 (0.37)	1.12 (0.17)	1.64 (0.52)	–	–	–
Acetone/propanal	C_3H_6O	0.69 (0.13)	2.07 (0.36)	0.62 (0.03)	1.13 (0.82)	–	–	0.37 (0.10)
Hydroxyacetone	$C_3H_6O_2$	–	1.35 (0.55)	0.90 (0.36)	1.13 (0.31)	–	–	–
Furan	C_4H_4O	–	0.55 (0.05)[d]	0.46 (0.05)[d]	0.51 (0.06)[d]	0.20 (0.21)	0.27 (0.19)	0.28 (0.03)
2,3-Butanedione	$C_4H_6O_2$	2.10 (0.63)	–	–	2.10 (0.63)	–	–	–
MVK/MACR /crotonaldehyde	C_4H_6O	–	0.37 (0.05)	0.29 (0.03)	0.33 (0.06)	–	–	–
Isoprene hydroperoxyaldehydes	$C_5O_3H_8$	–	0.18 (0.09)	0.16 (0.08)	0.17 (0.02)	–	–	–
Hydroxymethylhydrogenperoxide	CO_3H_4	–	0.33 (0.17)	0.048 (0.024)	0.19 (0.20)	–	–	–
Peroxyacetic acid/ hydroperoxy glycolaldehyde	$C_2O_3H_4$	–	0.44 (0.24)	0.045 (0.023)	0.24 (0.28)	–	–	–
Hydroperoxy acetone	$C_3O_3H_6$	–	0.13 (0.07)	0.043 (0.022)	0.086 (0.061)	–	–	–
C_4-dihydroxycarbonyls	$C_4O_3H_8$	–	0.075 (0.039)	0.020 (0.010)	0.047 (0.039)	–	–	–

Table 3. (continued)

Fire		Colockum Tarps	Big Windy Complex	Rim Fire	Study Average	Temperate Forests	Prescribed Fires in South Carolina	Boreal Forests
C_4-hydroxydicarbonyls/ C_5-alkenediols	$C_4O_3H_6$/ $C_5O_2H_{10}$	–	0.12 (0.06)	0.090 (0.045)	0.11 (0.02)	–	–	–
Isoprene hydroxy hydroperoxides/ isoprene epoxydiols	$C_5O_3H_{10}$	–	0.11 (0.04)	0.042 (0.013)	0.076 (0.047)	–	–	–
Ethane	C_2H_6	–	0.89 (0.06)	0.54 (0.04)	0.72 (0.25)	1.12 (0.67)	0.489 (0.359)	0.56 (0.13)
Ethene	C_2H_4	–	1.03 (0.08)	0.79 (0.06)	0.91 (0.17)	1.12 (0.35)	–	0.82 (0.09)
Ethyne	C_2H_2	–	0.26 (0.02)	0.21 (0.02)	0.24 (0.04)	0.29 (0.10)	–	0.22 (0.09)
Propane	C_3H_8	–	0.32 (0.02)	0.17 (0.01)	0.24 (0.11)	0.26 (0.11)	0.153 (0.099)	0.23 (0.05)
Propene	C_3H_6	–	0.36 (0.03)	0.35 (0.03)	0.35 (0.01)	0.95 (0.54)	–	0.38 (0.04)
i-Butane	C_4H_{10}	–	0.023 (0.002)	0.010 (0.001)	0.016 (0.009)	–	0.010 (0.005)	0.021 (0.004)
n-Butane	C_4H_{10}	–	0.084 (0.006)	0.038 (0.003)	0.061 (0.033)	0.083 (0.10)	0.036 (0.016)	0.076 (0.015)
1,2-Propadiene	C_3H_4	–	0.011 (0.002)	0.011 (0.002)	0.011 (0.000)	–	0.015 (0.002)	–
trans-2-Butene	C_4H_8	–	$2.2\ (0.2) \times 10^{-3}$	0.011 (0.002)	$6.8\ (6.5) \times 10^{-3}$	–	0.035 (0.018)	0.020 (0.003)
cis-2-Butene	C_4H_8	–	$2.0\ (0.3) \times 10^{-3}$	0.011 (0.002)	$6.7\ (6.7) \times 10^{-3}$	–	0.028 (0.016)	0.015 (0.002)
1-Butene	C_4H_8	–	0.079 (0.007)	0.080 (0.006)	0.080 (0.001)	–	0.131 (0.034)	0.077 (0.009)
i-Butene	C_4H_8	–	0.043 (0.004)	0.043 (0.004)	0.043 (0.000)	–	0.088 (0.017)	0.056 (0.007)
1,3-Butadiene	C_4H_6	–	0.043 (0.005)	0.067 (0.006)	0.055 (0.017)	–	–	0.070 (0.008)
i-Pentane	C_5H_{12}	–	0.016 (0.002)	$5.0\ (0.5) \times 10^{-3}$	0.010 (0.008)	–	0.007 (0.002)	0.019 (0.005)
n-Pentane	C_5H_{12}	–	0.043 (0.003)	0.017 (0.002)	0.030 (0.019)	–	0.019 (0.003)	0.042 (0.008)
1-Pentene	C_5H_{10}	–	0.029 (0.002)	0.022 (0.002)	0.026 (0.005)	–	0.030 (0.005)	–
Isoprene	C_5H_8	–	0.043 (0.007)	0.032 (0.003)	0.038 (0.007)	–	0.14 (0.03)	0.074 (0.017)
2,3-Dimethylbutane	C_6H_{14}	–	$1.4\ (0.1) \times 10^{-3}$	$5.0\ (0.6) \times 10^{-4}$	$9.6\ (6.4) \times 10^{-4}$	–	–	–
2 + 3-Methylpentane	C_6H_{14}	–	$8.2\ (0.6) \times 10^{-3}$	$4.0\ (0.3) \times 10^{-3}$	$6.1\ (4.7) \times 10^{-3}$	–	0.010 (0.002)	0.018 (0.004)
n-Hexane	C_6H_{14}	–	0.030 (0.002)	0.012 (0.001)	0.021 (0.012)	–	0.012 (0.003)	0.027 (0.006)
n-Heptane	C_7H_{16}	–	0.014 (0.001)	–	0.014 (0.001)	–	0.008 (0.005)	0.024 (0.004)
Benzene	C_6H_6	0.39 (0.11)	0.57 (0.04)[e]	0.34 (0.02)[e]	0.43 (0.12)	–	0.283 (0.043)	0.55 (0.11)
Toluene	C_7H_8	0.25 (0.06)	0.29 (0.02)[e]	0.20 (0.02)[e]	0.24 (0.05)	–	0.199 (0.031)	0.24 (0.06)
Ethylbenzene	C_8H_{10}	–	0.031 (0.003)	0.021 (0.002)	0.026 (0.007)	–	0.039 (0.016)	0.025 (0.009)
m + *p*-Xylene	C_8H_{10}	–	0.086 (0.009)	0.085 (0.010)	0.086 (0.001)	–	0.080 (0.055)	0.060 (0.008)
o-Xylene	C_8H_{10}	–	0.040 (0.004)	0.036 (0.004)	0.038 (0.003)	–	0.025 (0.011)	0.027 (0.003)
α-Pinene	$C_{10}H_{16}$	–	0.017 (0.002)	0.018 (0.002)	0.017 (0.001)	–	0.094 (0.021)	0.81 (0.10)
β-Pinene	$C_{10}H_{16}$	–	0.014 (0.003)	0.006 (0.001)	0.010 (0.006)	–	0.052 (0.013)	0.72 (0.09)
Monoterpenes	$C_{10}H_{16}$	–	0.45 (0.08)	0.37 (0.07)	0.41 (0.06)	–	1.61 (1.00)	–
Ammonium	NH_4	0.19 (0.12)	0.49 (0.17)	0.34 (0.12)	0.34 (0.15)	–	–	–
Nitrate	NO_3	0.73 (0.42)	0.99 (0.34)	0.90 (0.31)	0.87 (0.13)	–	–	–
Chloride	Chl	0.42 (0.12)	0.064 (0.022)	0.082 (0.029)	0.19 (0.20)	–	–	–
Sulfate	SO_4	0.46 (0.10)	0.15 (0.05)	0.29 (0.10)	0.30 (0.16)	–	–	–
Organic aerosol	OA	23.3 (4.76)	30.9 (11.8)	18.8 (7.3)	24.3 (6.1)	–	–	–
Submicron aerosol	PM_1	25.1 (4.8)	32.6 (11.8)	20.4 (7.3)	26.0 (6.2)	12.7 (7.5)[f]	–	–

[a]Values in parenthesis are errors for single fire and standard deviations for all available EFs for study averages.
[b]HFCs and HCFCs are purely anthropogenic compounds that are not expected from BB.
[c]NO_x emission from the Big Windy Complex is likely much larger (see text).
[d]EF for furan/pentadienes/cyclopentene, determined as the deference between PTR-MS measured isoprene/furan/pentadienes/cyclopentene and WAS measured isoprene.
[e]Reported as PTR-MS and WAS averages.
[f]Reported as $PM_{2.5}$-$PM_{3.5}$.

discussion of the emissions of different compounds and their comparison with these previous airborne measurements is presented below.

3.1.1. Sulfur Compounds

SO_2 was the main sulfur-containing gas measured from the three fires, followed by significantly less dimethyl sulfide (DMS) and carbonyl sulfide (OCS). The study average EF(SO_2) (0.32 ± 0.37 g kg^{-1}) is smaller than the average EF(SO_2) (2.03 ± 1.79 g kg^{-1}) for various temperate evergreen fires [*Akagi et al.*, 2011] and (0.795 ± 0.377 g kg^{-1}) for 15 agricultural fires sampled during SEAC^{4}RS [*Liu et al.*, 2016], though the differences are not statistically significant. Note that the uncertainty in the SO_2 EF is large because it represents

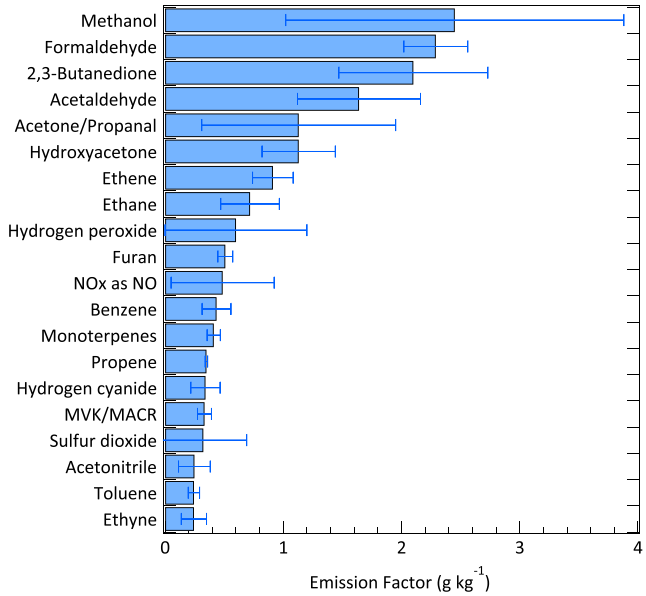

Figure 2. The average emission factors (boxes) and standard deviations (whiskers) for the 20 most abundant trace gases (excluding CO_2, CO, and CH_4) measured from the three wildfires.

fire-to-fire variability, whereas the uncertainty in the EF for each individual fire is tightly constrained (Table 3). Since SO_2 emissions are found to be highly dependent on fuel sulfur content [*Burling et al.*, 2010; *Stockwell et al.*, 2014], the reason for our low EF(SO_2) relative to other studies is presumably lower sulfur content for the plants burned, especially for those burned in the two SEAC^{4}RS fires. Since there could be SO_2 oxidation to particulate sulfate given high levels of H_2O_2 in the SEAC^{4}RS plumes, summing up the emitted SO_2 and sulfate may better reflect fuel sulfur content. The resulting combined sulfur emissions from the SEAC^{4}RS fires (0.21–0.31 g kg^{-1}) were still lower than the above-cited average SO_2 EFs.

DMS was clearly released from the two SEAC^{4}RS fires as it was strongly correlated with CO ($r^2 > 0.97$). OCS was also highly correlated with CO for the Rim Fire ($r^2 = 0.91$). However, OCS from the Big Windy Complex had no measurable elevation and weak correlation with excess CO ($r^2 = 0.14$). Both DMS and OCS have been measured previously from prescribed [*Akagi et al.*, 2013] and boreal forest fire plumes [*Yokelson et al.*, 1997; *Simpson et al.*, 2011] with EFs ranging 0.0023–0.008 g kg^{-1} and 0.01–0.029 g kg^{-1}, respectively (Table 3). While the Big Windy Complex EF(DMS) (0.0057 ± 0.0012 g kg^{-1}) is within the range observed from the few available studies, the Rim Fire EF(DMS) (0.00056 ± 0.00012) and EF(OCS) (0.0059 ± 0.0009) are both lower than the literature values.

3.1.2. Chlorine Compounds and Halocarbons

The chlorine-containing gases emitted from the two SEAC^{4}RS fires are HCl and six halocarbons, methyl chloride (CH_3Cl), dichloromethane (CH_2Cl_2), 1,2-dichloroethane, methyl iodide (CH_3I), methyl bromide (CH_3Br), and dibromomethane (CH_2Br_2). In addition, hydrochlorofluororcarbon (HCFC)-142b, HCFC-141b, and hydrofluorocarbon (HFC)-152a were also measurably enhanced in the plumes, as discussed below. The HCl emission was very low, with an average EF of 0.0039 ± 0.0010 g kg^{-1}. This value is almost the smallest of the existing HCl emissions from various fuel types burned in field or laboratory, which range from 0.008 to 3.61 g kg^{-1} [*Akagi et al.*, 2011; *Stockwell et al.*, 2014]. As also shown in Table 3, particulate chloride EFs from these two fires (0.064–0.082 g kg^{-1}) were near the lower end of a range of EFs from prescribed fires of different ecosystems (0.13 to 1.3 g kg^{-1}) [*May et al.*, 2014]. HCl and chloride emissions were found in laboratory studies to have a significant dependence on fuel composition for a variety of biomass fuels [*Christian et al.*, 2003; *Hosseini et al.*, 2013; *Stockwell et al.*, 2014]. For example, oak, one of the fuels burned in the two SEAC^{4}RS fires, was found to have low Cl content and low EF(chloride) when compared to some other southwestern U.S. fuels [*Hosseini et al.*, 2013]. Thus, low EFs of HCl and chloride observed in these two fires may imply a low chlorine fraction of the fuels burned.

The nine halocarbons included in Table 3 showed reasonable correlations with CO ($0.61 < r^2 < 0.99$) and measurable enhancements compared to the background air. The emissions of CH_3Cl, CH_3I, CH_3Br, CH_2Br_2, and 1,2-dichloroethane have been previously reported by *Simpson et al*. [2011] from Canadian forest fire plumes. Except for a factor of 4 higher value of EF(CH_2Br_2) and a factor of 2 lower value of CH_3Br, the average EFs measured in this work are similar to (within 5–28% of) those reported by *Simpson et al*. [2011]. In addition, CH_2Cl_2 was also emitted with an average ER to CO of $(4.0 \pm 1.8) \times 10^{-6}$, which is in between the ERs $< (1–6) \times 10^{-7}$ measured in Tasmania [*Simmonds et al*., 2006] and the ER = $(2.5 \pm 0.6) \times 10^{-5}$ measured in Africa [*Rudolph et al*., 1995]. Note that the more smoldering Big Windy Complex consistently emitted more of these halocarbons than the Rim Fire. Methyl halides (CH_3Cl, CH_3Br, and CH_3I) are thought to form predominantly from smoldering and also reflect halogen content in fuels burned [*Reinhardt and Ward*, 1995; *Andreae and Merlet*, 2001]. It is also known that in the Pacific Northwest, chlorine and bromine concentrations in vegetation decrease with distance from the coast [*McKenzie et al*., 1996]. Therefore, both the burning condition and the closer proximity to ocean could possibly account for higher halocarbon emissions from the Big Windy Complex.

HFCs, CFCs, and HCFCs are produced exclusively by anthropogenic activities and are not expected from BB. A possible explanation for their enhanced concentrations in the wildfire plumes could be a re-suspension after being deposited previously onto the forests. *Hegg et al*. [1990] also observed variable CFC-12 (CF_2Cl_2) emissions from seven fires in North America, most pronounced in the Los Angeles basin. In contrast, *Simpson et al*. [2011] did not see any elevated HFCs or HCFCs over remote regions of Canada. Our observations may suggest the deposition of HFCs and HCFCs on vegetation in the regions studied. However, since these compounds are highly volatile, their enhancements in wildfire plumes may result from other unknown mechanisms.

3.1.3. Nitrogen Compounds

Freshly emitted gaseous nitrogen-containing compounds measured in the plumes are (in descending EF order) nitrogen dioxide (NO_2), HCN, CH_3CN, nitrogen monoxide (NO), multifunctional organic nitrates usually derived from the oxidation of isoprene and other alkenes [*Paulot et al*., 2009a; *Lee et al*., 2014; *Teng et al*., 2015], and C_1–C_5 saturated alkyl nitrates. Similar to many other BB studies [*Yokelson et al*., 2009; *Alvarado et al*., 2010; *Liu et al*., 2016], the observed nitric acid (HNO_3) was not significantly elevated within the fresh wildfire plumes.

Since NO and NO_2 are rapidly interconverted, it is also useful to report an EF for NO_x as NO. In Table 3, the derived EFs of NO, NO_2, and NO_x from the three wildfires are all the smallest among the studies listed. The Big Windy Complex emitted extremely small amounts of NO_x (0.067 ± 0.008 g kg^{-1}). One reason could be that the smoldering dominated burning conditions did not favor NO_x emission [*Lobert et al*., 1991; *Yokelson et al*., 1996; *Goode et al*., 2000]. However, as the samples of the Big Windy Complex and the Rim Fire included smoke up to ~1–2 h old, the freshly emitted NO_x might have partially transformed to other reactive nitrogen species such as PAN and particulate nitrate. In support of this, elevated PAN was observed for both fires, while a decrease in $\Delta NO_x/\Delta CO$ was seen in the Rim Fire plume as the distance from the fire source increased. Adding in the observed PAN to NO_x would enhance the NO_x emissions by ~5 times and by 29% for the Big Windy Complex and the Rim Fire, respectively. For this reason, the NO_x emissions from the Big Windy Complex are significantly underestimated.

HCN and CH_3CN are commonly recognized as BB tracers, and their ER, $\Delta CH_3CN/\Delta HCN$, ranges between 0.30 and 0.56 for a wide range of fuels burned in the laboratory and field [*Li et al*., 2000; *Christian et al*., 2003; *de Gouw et al*., 2003; *Yokelson et al*., 2008; *Crounse et al*., 2009; *Yokelson et al*., 2009; *Simpson et al*., 2011]. Our CH_3CN/HCN ratio is about 0.3 for fires where both species were measured. The average EF(HCN), 0.34 ± 0.12 g kg^{-1}, from the two SEAC^{4}RS fires is low compared to the other forest fires listed in Table 3 (0.66–0.89 g kg^{-1}). Note that the small uncertainty we report, 0.12 g kg^{-1}, only reflects the standard deviation of the two SEAC^{4}RS EFs, whereas the measurement uncertainty is actually as high as 50%. Previously, forest fire CH_3CN emissions were measured mostly from boreal and tropical regions but rarely from temperate regions [*Akagi et al*., 2011; *Simpson et al*., 2011; *Müller et al*., 2016]. A typical range for forest fire CH_3CN EFs in the literature is 0.2 to 0.6 g kg^{-1}. While the CH_3CN emission from the Rim Fire (EF = 0.13 ± 0.02 g kg^{-1}) was below this range, those from the other two fires are both within it. Note that the Rim Fire also had a relatively low EF(HCN) of 0.25 ± 0.13 g kg^{-1}. A recent study of BB emissions demonstrated that HCN and CH_3CN

emissions are nonlinearly dependent on the nitrogen level of the fuel [*Coggon et al*., 2016]. The ERs of $\Delta CH_3CN/\Delta HCN$ for the two SEAC^{4}RS fires, 0.31 and 0.35, are at the lower end of the generally observed range, 0.30–0.56, as noted above.

Alkyl nitrate formation is an important feature of NO_x–VOC chemistry, and it also affects organic aerosol (OA) formation [*Perring et al*., 2013; *Lee et al*., 2016]. In general, the average EFs of the saturated C_1–C_5 alkyl nitrates from the two SEAC^{4}RS wildfires are similar to those measured from boreal forest fire plumes [*Akagi et al*., 2011; *Simpson et al*., 2011]. In addition, we report the first EFs of multifunctional organic nitrates (isoprene/butadiene/butene/propene/ethene hydroxynitrates, methyl vinyl ketone/methacrolein hydroxynitrates, propanone nitrate, ethanal nitrate, and nitroxyhydroperoxide + nitroxyhydroxyepoxide) from BB. In the fresh plumes of the two SEAC^{4}RS fires, most of these nitrates were elevated over background by less than 200 pptv, corresponding to ERs to CO on the order of 10^{-6}–10^{-5}. Although relatively minor in concentrations, they exhibit excellent correlations with HCN with r^2 generally larger than 0.95, indicating a clear BB source. The summed emissions of these measured alkyl nitrates are 0.18 g kg^{-1} (8.5% of HCN by molar ratio) and 0.12 g kg^{-1} (9.6% of HCN by molar ratio) for the Big Windy Complex and the Rim Fire, respectively.

3.1.4. Nonmethane Organic Compounds

Open biomass burning is the second largest global source of gas-phase NMOCs after biogenic emissions [*Yokelson et al*., 2008]. The emitted NMOCs can greatly influence the production of ozone and secondary organic compounds. Additional NMOCs, especially OVOCs, have been measured by recent work, which can then improve photochemical model performance [*Stockwell et al*., 2015; *Liu et al*., 2016; *Müller et al*., 2016]. The extensive measurements during SEAC^{4}RS enable the development of a detailed set of EFs of NMOCs for wildfires. The PTR-MS on board the G-1 aircraft also measured several important NMOCs from the Colockum Tarps fire. Among the common species, the Big Windy Complex had higher emissions for a variety of OVOCs measured by PTR-MS and CIMS. Its smoldering dominated burning condition could have contributed to the higher OVOC EFs, although this observation cannot be fully explained without knowing differences in fuels.

The most abundant NMOCs emitted from the wildfires are methanol, formaldehyde, acetaldehyde, acetone/propanal, and hydroxyacetone. They are also often the most abundant OVOCs emitted by other types of BB [*Akagi et al*., 2011; *Stockwell et al*., 2014, 2015; *Liu et al*., 2016]. Although not measured here, acetic acid is often another major NMOC emitted from forest fires [*Akagi et al*., 2011; *Yokelson et al*., 2013]. In general, our average EFs of the measured compounds (except for hydroxyacetone) agree within a factor of ~2 with the other studies listed in Table 3 and from burning different plants as compiled by *Akagi et al*. [2011]. Hydroxyacetone emissions from a prescribed forest fire have recently been reported by *Müller et al*. [2016] with an average EF of 0.28 ± 0.15 g kg^{-1}. The two SEAC^{4}RS fires produced relatively high amounts of hydroxyacetone, with an average EF of 1.13 ± 0.31 g kg^{-1}, which is higher than those for a variety of common fire types studied during the fourth Fire Lab at Missoula Experiment (FLAME-4) except for crop residue fuels.

2,3-butanedione has been found to be an important precursor of peroxyacetyl radicals through photolysis and has large effects on modeled plume chemistry [*Liu et al*., 2016; *Müller et al*., 2016]. We report an EF(2,3-butanedione) of 2.10 ± 0.63 g kg^{-1} for the Colockum Tarps fire, which was the second most abundant NMOC after formaldehyde for that fire, even higher than methanol and acetaldehyde. This EF is much higher than the measured 0.44 ± 0.18 g kg^{-1} from a small prescribed fire in Georgia [*Müller et al*., 2016], 0.73 ± 0.22 g kg^{-1} for some tropical deforestation fires [*Yokelson et al*., 2008], and ~0.2–1.2 g kg^{-1} for a variety of fuels burned in laboratory fires [*Yokelson et al*., 2008; *Stockwell et al*., 2015]. Such high primary 2,3-butanedione emissions significantly promote peroxyacetyl nitrate (PAN) formation in downwind plumes.

The SEAC^{4}RS data extend previously published emissions by including a few OVOCs that are also important products from the oxidation of biogenic emissions such as isoprene [*Paulot et al*., 2009a, 2009b; *Crounse et al*., 2011, 2013; *Bates et al*., 2016]. These species consist of peroxyacetic acid (PAA) and hydroperoxy glycolaldehyde (HPGLYC), hydroperoxy acetone, organic peroxides (hydroxymethylhydrogenperoxide (HMHP) and isoprene hydroxy hydroperoxides and epoxydiols), isoprene hydroperoxyaldehydes (HPALDs), and some other hydroxy compounds (C_4-dihydroxycarbonyls, C_4-hydroxydicarbonyls, and C_5-alkenediols). These intermediate compounds are of particular interest because they are known to affect the atmosphere's oxidative capacity and form secondary organic aerosol (SOA) [*Lelieveld et al*., 2008; *Surratt et al*., 2010]. PAA/HPGLYC, HMHP, and HPALDs are the three compounds that had the highest average EFs: 0.24 ± 0.28, 0.19 ± 0.20, and

0.17 ± 0.02 g kg^{-1}. HPALDs were also found to be abundant in agricultural fire plumes, with a higher average EF of 0.406 ± 0.229 g kg^{-1} [*Liu et al.*, 2016]. While the EF(HPALD) values were similar for the Big Windy Complex and Rim Fire, EF(PAA/HPGLYC) and EF(HMHP) showed strong fire-to-fire variability, with EFs 7–10 times higher from the Big Windy Complex.

Among the nonmethane hydrocarbons (NMHCs) quantified from the SEAC^{4}RS fires, the shorter-chained alkanes and alkenes (C_2–C_3) were most abundant in the plumes on a molar basis, as was also found in other BB studies [*Akagi et al.*, 2011; *Simpson et al.*, 2011]. Benzene and toluene ranked highest among the longer-chained hydrocarbons ($\geq C_4$) based on both ERs and EFs. Most of the NMHC EFs were comparable to the other forest fires listed in Table 3. The NMHCs that had lower EFs for both the two SEAC^{4}RS fires than some literature values are mainly terpenes including isoprene, α-pinene, β-pinene, and total monoterpenes. The average EF(α-pinene) and EF(β-pinene) in this study are lower by over 5 times and 40 times than those obtained from prescribed forest fires in South Carolina [*Akagi et al.*, 2013] and boreal forest fires in Canada [*Simpson et al.*, 2011], respectively. The highest pinene EFs from the boreal forest fires is consistent with their stronger association with coniferous than deciduous ecosystems [*Fuentes et al.*, 2000]. However, since western forests burned here are also predominantly coniferous, vegetation type alone may not account for the difference in pinene emissions. Additionally, *Akagi et al.* [2013] suggests that α-pinene and β-pinene may be preferentially released from fuels on the ground (duff, dead-down woody fuels, etc.) that burn largely by RSC, and temperate forests tend to have a smaller loading of dead-down woody fuels than boreal forests. Compared to the boreal fire plumes, the lower EF(pinenes) determined here may be partially explained by the fact that less emissions from such fuels were lofted and sampled, possibly due to previous burns and thinning operations in the case of the Rim Fire. However, other factors such as fire variability and photochemical processing are also expected to contribute to the difference.

3.2. Initial Emissions of PM_1

PM emissions from temperate fuels have been measured mainly from prescribed fires and in laboratory studies [*Hosseini et al.*, 2013; *May et al.*, 2014]. Very recently, *Collier et al.* [2016] reported aerosol enhancement ratios from 32 wildfire plumes originating from the Pacific Northwest region during BBOP, which were sampled at a fixed site located in central Oregon as well as from the G-1 aircraft. In addition, BB OA has been shown to contain substantial amounts of light-absorbing brown carbon (BrC), which has potential impacts on climate forcing [*Saleh et al.*, 2013; *Forrister et al.*, 2015; *Washenfelder et al.*, 2015; *Liu et al.*, 2016]. *Forrister et al.* [2015] presented a detailed examination of BrC evolution in the smoke of the Rim Fire. Here we report a suite of emissions of nonrefractory components of PM_1 from western wildfires measured by the aerosol mass spectrometer (AMS). It is known that the measured fine PM emissions for similar fuel types often vary between field-measured prescribed burns and laboratory-based burns due to different burning control and fuel conditions such as moisture content [*May et al.*, 2014]. Similarly, fine PM variability may also exist between prescribed fires and uncontrolled wildfires, which tend to burn at lower fuel moisture. However, little information is available for a detailed comparison. Therefore, we also compare our EF(PM_1) with previous airborne and ground-based studies that measured the same PM_1 species from prescribed fires (Table 4).

The major particulate species emitted from all three fires are OA, with an average EF of 24.3 ± 6.1 g kg^{-1} (Table 3). The Big Windy Complex had the largest EF(OA) among the three studied fires (30.9 ± 11.8 g kg^{-1}). This high EF(OA) was possibly related to the smoldering burning conditions, although it could also be affected by gas-particle partitioning of semivolatile compounds during the dilution processes. Another complication is the net formation of secondary OA (SOA) that could contribute to higher downwind ΔOA/ΔCO, which could be important for the SEAC^{4}RS plumes as they involved smoke as old as 1–2 h. Highly variable SOA formation rates in aging BB plumes have been reported, although limited net increase in OA mass has often been observed [*Capes et al.*, 2008; *Yokelson et al.*, 2009; *Cubison et al.*, 2011; *Liu et al.*, 2016]. In the case of the Rim Fire, besides the relatively fresh plumes (~20–120 min), there were also samples >4 h old. We found that in the fresh Rim Fire plumes that ranged from ~20 to 120 min old, ΔOA/ΔCO and the oxygen-to-carbon (O/C) ratio remained at 0.24 g g^{-1} and ~0.5, respectively, without significant variation. In contrast, in the ~4 h old plumes, ΔOA/ΔCO decreased to 0.11 g g^{-1}, while the average O/C ratio increased to ~0.8. This indicated that between ~2 and 4 h, the net effect of oxidation and evaporation resulted in a 54% decrease in OA mass. *Forrister et al.* [2015] found that ΔOA/ΔCO exhibited little change afterward in more

Table 4. Comparison of Aerosol EFs (g kg^{-1}) and ERs to $\Delta(CO_2 + CO)$ for Temperate Fuels Measured From Aircraft

Fire	Western Wildfires (This Work)		Prescribed Chaparral Fires [*May et al.*, 2014]	Prescribed Montane Fires [*May et al.*, 2014]	Prescribed SE Coastal Plain Fires [*May et al.*, 2014]	Western Wildfires [*Collier et al.*, 2016]
MCE	0.912 (0.031)		0.924 (0.019)	0.899 (0.020)	0.936 (0.014)	0.91 (0.046)
	EF (g kg^{-1})	ER to $\Delta(CO_2 + CO)$ ($\mu g\ m^{-3}\ ppm^{-1}$)	EF (g kg^{-1})	EF (g kg^{-1})	EF (g kg^{-1})	ER to $\Delta(CO_2 + CO)$ ($\mu g\ m^{-3}\ ppm^{-1}$)
OA	24.3 (6.1)	30.0 (8.1)	3.9 (1.8)	11.2 (2.7)	2.8 (1.6)	31 (24)
BC	-	-	1.43 (0.13)	0.59 (0.13)	1.11 (0.67)	-
NH_4	0.34 (0.15)	0.42 (0.19)	0.05 (0.05)	0.06 (0.00)	0.07 (0.03)	0.32 (0.32)
NO_3	0.87 (0.13)	1.08 (0.18)	0.08 (0.07)	0.20 (0.00)	0.09 (0.03)	0.81 (0.94)
Chl	0.19 (0.20)	0.23 (0.24)	0.08 (0.05)	0.01 (0.00)	0.09 (0.15)	-
SO_4	0.30 (0.16)	0.37 (0.18)	0.01 (0.01)	0.01 (0.00)	0.17 (0.10)	-
PM_1	26.0 (6.2)	32.1 (8.2)	5.5 (1.7)	12.1 (2.9)	4.4 (2.0)	-

aged Rim Fire plumes up to ~50 h. Similarly, constant ΔOA/ΔCO and O/C ratio were also seen in the fresh Big Windy Complex plumes. Therefore, the OA EFs in this study represent freshly emitted OA (< 2 h) that did not undergo a significant change in mass due to aging. As noted below, the higher initial emissions from wildfires are important despite the decrease in OA/CO with aging observed in the Rim Fire.

For all three fires, OA emissions represented the majority of the mass (>90%) of the emitted PM_1. Such a high OA fraction was also observed from montane prescribed fires and from burning pines and dense fuels such as duff and peat in laboratory studies [*May et al.*, 2014]. Based on aircraft observations, *May et al.* [2014] observed significantly smaller EF(OA) in young plumes up to 2 h emitted from prescribed fires for three temperate ecosystems, namely, maritime chaparral (3.9 ± 1.8 g kg^{-1}), montane (11.2 ± 2.7 g kg^{-1}), and southeastern coastal plain (2.8 ± 1.6 g kg^{-1}). By contrast, by calculating enhancement ratios as $\Delta OA/\Delta(CO_2 + CO)$, we find that our average value, 30.0 ± 8.1 $\mu g\ m^{-3}\ ppm^{-1}$, agrees well with the average of 31 ± 24 $\mu g\ m^{-3}\ ppm^{-1}$ for the 32 wildfire plumes reported by *Collier et al.* [2016]. It is significant to note that the plumes sampled in that study included many that aged beyond 2–4 h. Thus, the net decrease in mass after emission observed for the Rim Fire may be unusual. *Cubison et al.* [2011] and *Jolleys et al.* [2012, 2015] summarize some field BB data sets for boreal and tropical wildfires and conclude that fresh ΔOA/ΔCO often ranged from ~0.02 to 0.33 g g^{-1}. In this study, the ERs of ΔOA/ΔCO for the three fires ranged between 0.24 and 0.34 g g^{-1}, which lies in the upper end of the previously reported range.

The dominant inorganic aerosol species measured by the AMS are ammonium, nitrate, chloride, and sulfate, with average EFs of 0.34 ± 0.15, 0.87 ± 0.13, 0.19 ± 0.20, and 0.30 ± 0.16 g kg^{-1}. All these average EFs are larger than the aircraft-measured EFs from U.S. prescribed fires reported by *May et al.* [2014] (Table 4). For tropical forest fires, wide ranges of sulfate (~0.05–0.21 g kg^{-1}) and chloride (~0.07–0.51 g kg^{-1}) EFs have been measured in the field [*Yokelson et al.*, 2009; *Akagi et al.*, 2011]. Compared to the tropical fires, our average EF(sulfate) is relatively high, while the average EF(chloride) is within the observed range of chloride emissions. Nitrate and ammonium are often found to be minor components of the emitted nitrogen species when compared to NO_x and NH_3 from various BB studies, with EFs generally less than ~0.2 g kg^{-1} [*McMeeking et al.*, 2009; *Akagi et al.*, 2011]. In our work, the emitted nitrogen as nitrate and ammonium accounted for 87% and 116% of that as NO_x on average, respectively. Note that although nitrate and ammonium have been observed in primary fine PM (e.g., *Lewis et al.* [2009]), our observations may also include some secondary production, since NO_x conversion to PAN was observed in the Big Windy Complex and the Rim Fire plumes. *Collier et al.* [2016] also observed significant nitrate and ammonium emissions, which were both ~25% lower than our observations based in ERs to $\Delta(CO_2 + CO)$.

We combined our EF measurements of nonrefractory species to investigate the total PM_1 emission from the temperate wildfires. The average EF(PM_1) for the three fires is 26.0 ± 6.2 g kg^{-1}, which is more than 2 times larger than the average for the montane prescribed fires and ~5–6 times larger than those for the chaparral and coastal plain fires (Table 4). Although black carbon (BC) is not included in our EF(PM_1), we expect the comparison to be roughly the same since our EF(PM_1) is dominated by OA. Our EF(PM_1) is also substantially larger than the temperate forest average reviewed by *Akagi et al.* [2011], which takes into account two wildfires and many prescribed fires (Table 3). Although the analysis is limited, our overall higher EF(PM_1) may

reflect differences between emissions from prescribed fires and wildfires due to differences in fuel content and condition, burning condition, and fire size and intensity. For example, inorganic EFs are often found to have a strong dependence on fuel composition [*Christian et al*., 2003; *Burling et al*., 2010; *May et al*., 2014] and OA is mainly produced by smoldering combustion [*Reid et al*., 2005]. Since the observed wildfire MCEs of both this work and *Collier et al*. [2016] fall within the range of MCEs that is commonly measured for prescribed fires (Table 4), other reasons besides the smoldering to flaming ratio of the fire are needed to explain the higher production of OA from wildfires. For example, prescribed fires often occur within restricted meteorological and fuel moisture conditions designed to maintain containment of the fire while still burning a significant fraction of the fuel [*Radke et al*., 1991]. Different conditions that drive the wildfire intensity and movement may result in different PM EFs. In addition, wildfires tend to burn more dead/down fuels and live, moist canopy fuels, both of which can promote high OA emissions [*Yokelson et al*., 2008; *May et al*., 2014]. In short, this work suggests that the aircraft-measured EF(PM_1) from wildfires is more than 2 times that of prescribed fires.

In addition, wildfires typically consume more fuel than prescribed fires [*Campbell et al*., 2007; *Turetsky et al*., 2011; *Yokelson et al*., 2013]. Higher PM EFs and higher fuel consumption for wildfires suggest that it is possible to reduce overall PM emissions by prescribed burning. However, this assumes that prescribed burning will significantly reduce the prevalence of wildfires.

3.3. Relationship Between EF and MCE

BB emissions often vary with different combustion processes such as flaming and smoldering. For this reason, we examined the correlation between MCEs and the derived EFs for the three wildfires sampled in this study. Since BB studies for similar western fuels are rare, we also compare our data to the previous U.S. prescribed fire and boreal fire studies of *Burling et al*. [2011], *Simpson et al*. [2011], *Akagi et al*. [2013], and *May et al*. [2014]. The species we chose are CH_4, 16 out of the 20 most abundant gases in Figure 2, and the 5 PM_1 components, all of which comprise at least three data points obtained from this work and/or the selected prescribed fire studies. Despite differences in fuels and burning environments in these studies, we examined EFs as a function of MCE using all available data to provide a general idea about whether variability in MCE alone can describe the variability in EFs.

Figure 3 shows all gaseous species with a linear regression slope significantly different from 0, including NO_x, CH_4, methanol, benzene, toluene, formaldehyde, furan, and propene. EF(NO_x) increases as MCE increases, consistent with its primary emission from flaming combustion [*Yokelson et al*., 1996; *Lobert et al*., 1999; *Goode et al*., 2000]. All NMOCs in Figure 3 are negatively correlated with MCE, consistent with their emission from smoldering combustion. Variability in the EF versus MCE relationship does exist among the different studies. For example, the EF(NO_x) and MCE correlation ($r^2 = 0.29$) might have been degraded by other factors such as fuel nitrogen content [*McMeeking et al*., 2009; *Burling et al*., 2010] and photochemical aging. In addition, the EFs for propene from this work and *Simpson et al*. [2011] clearly lie below the overall fit and all other EFs at a similar MCE range (0.87–0.93).

Ethane, ethene, ethyne, HCN, CH_3CN, SO_2, acetone/propanal, MVK/MACR, and acetaldehyde are associated with EF-versus-MCE slopes that are not significantly different from 0 (Figure S4). For these species, data from different studies are more scattered. Ethane, ethene, HCN, CH_3CN, acetone, MVK/MACR, and acetaldehyde are primarily released from smoldering combustion [*McMeeking et al*., 2009; *Burling et al*., 2011; *Akagi et al*., 2013]. Except for CH_3CN and MVK/MACR, the EFs of these species showed negative correlations, however not strong, with MCE ($r^2 \leq 0.55$). SO_2 has been established as a flaming combustion product [*Yokelson et al*., 1996; *Andreae and Merlet*, 2001]. In agreement with this, the slope of our linear fit of EF(SO_2) as a function of MCE is positive, although not significant. The unexplained variability in EF(SO_2) may partly be due to the influence of fuel sulfur content and possible oxidation. Ethyne also has a positive slope ($r^2 = 0.09$), and it has been known as a product of both flaming and smoldering combustion [*Yokelson et al*., 2008; *Burling et al*., 2011; *Yokelson et al*., 2011].

PM_1 components emitted from wildfires generally follow their own separate and higher trend lines (Figure 4). When plotted with prescribed fire data, OA is the only component that had a slope significantly different from 0, which is negative and signifies production mainly by smoldering combustion. Inorganic PM_1 EFs are less dependent on MCE and likely more dependent on fuel composition. As shown by the regression results,

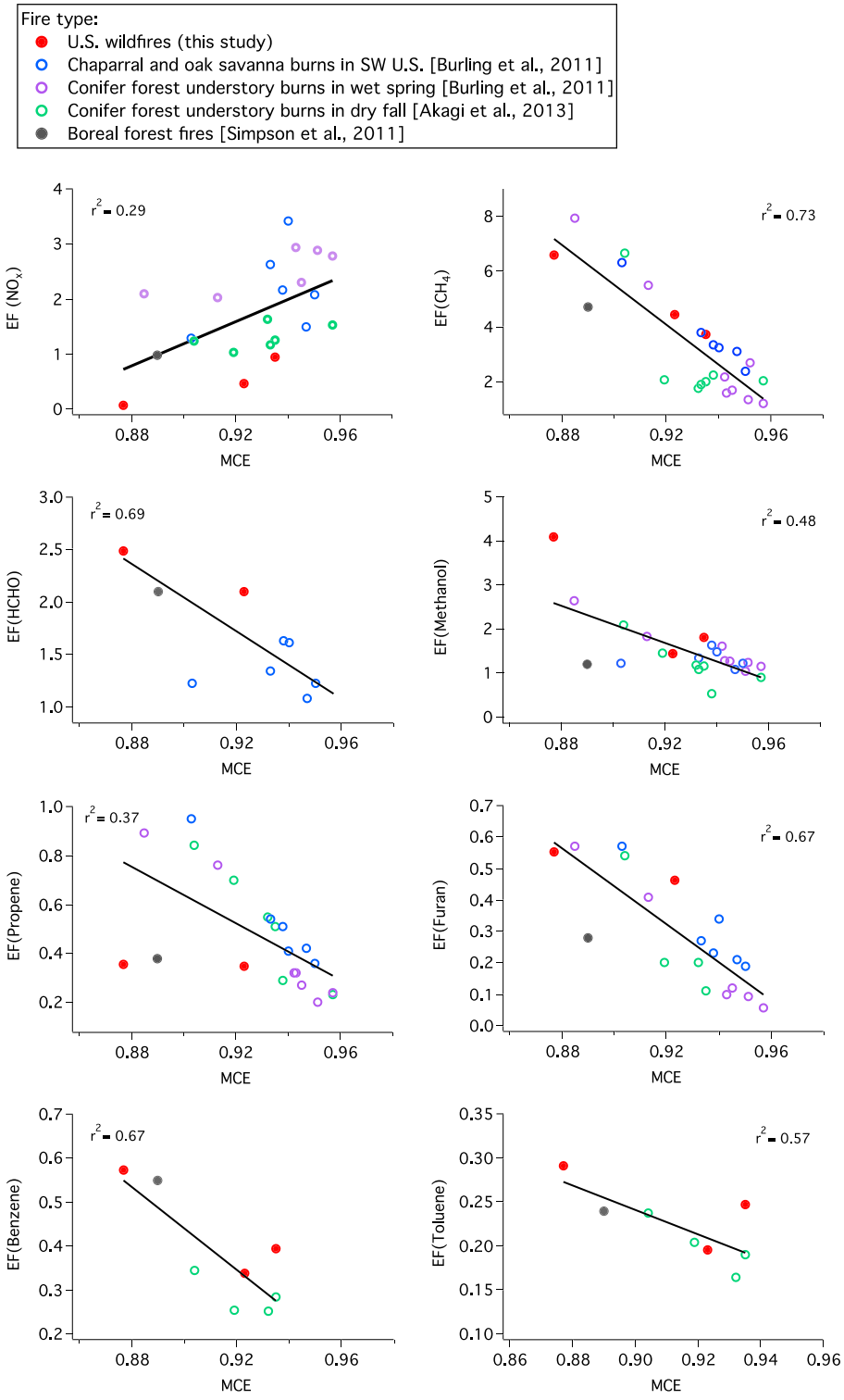

Figure 3. Emission factors (g kg^{-1}) of gaseous species as a function of MCE for the three wildfires of this study, the boreal forest fires of *Simpson et al.* [2011], and the prescribed fires of *Burling et al.* [2011] and *Akagi et al.* [2013]. Gases shown here are associated with slopes that are significantly different from 0. Correlation coefficients (r^2) were derived from bivariate linear regressions of all plotted data.

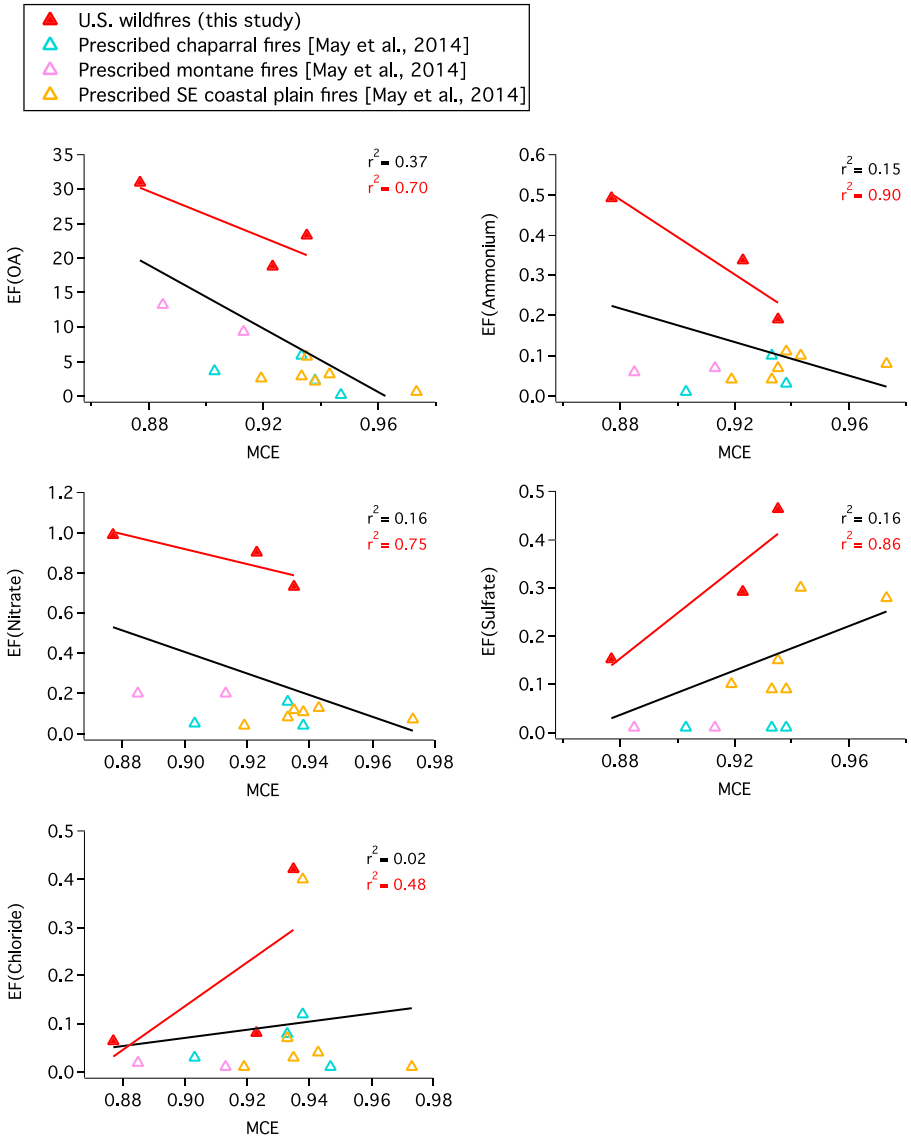

Figure 4. Emission factors (g kg^{-1}) of all fine particle species as a function of MCE for the three wildfires of this study and the prescribed fire data of *May et al.* [2014]. Correlation coefficients (r^2) were derived from bivariate linear regressions of all plotted data (black) and of data from this study (red). When fitted with prescribed fire data, only the slope of EF(OA) versus MCE is significantly different from 0.

numerous factors could affect the variability in emissions, which limits the predictive power of the EF and MCE relationship.

3.4. Emission Estimates From Western U.S. Wildfires

We used the measured EFs to estimate the annual emissions of CO, NO_x, SO_2, total NMOC, and PM_1 from wildfires in the western contiguous U.S. (defined here as 11 states: Arizona, California, Colorado, Idaho, Montana, Nevada, New Mexico, Oregon, Utah, Washington, and Wyoming). The wildfire season in the western U.S. is June–October [*Urbanski*, 2013]. Thus, the EFs of this study, which were derived within the wildfire season, may serve as reasonable estimates for typical wildfires in the western region. BB emissions are typically estimated as the product of EF, area burned, and fuel consumption per unit area [*Seiler and Crutzen*, 1980]. The burned area by state from 2011 to 2015 was obtained from the National Interagency Fire Center (NIFC; http://www.nifc.gov/fireInfo/fireInfo_statistics.html). Fuel consumption depends on the biomass available to burn and the fraction of biomass consumed by fire. Fuel consumption likely varies

Table 5. Area Burned (ha) and Estimated Annual Emissions (Gg yr^{-1}) by Western U.S. Wildfires

	This Work	NEI Wildfire	NEI All Other Sources	This Work Wildfire/NEI Wildfire	This Work Wildfire/NEI All Other Sources
Year	2011–2015	2011	2011	-	-
Area burned	1,698,115[a]	1,762,654	-	0.96	-
Emission by species					
CO	5,240 (2,240)	4,894	13,222	1.07	0.40
NO_x as NO_2	44 (41)	62	2,588	0.71	0.02
SO_2	19 (22)	35	352	0.54	0.05
NMOC	905 (437)[b]	1,153	14,361	0.78	0.06
PM_1 or $PM_{2.5}$ [c]	1,530 (570)	418	858	3.66	1.78

[a]Source: NIFC, http://www.Nifc.Gov/fireInfo/fireInfo_statistics.Html.
[b]Identified NMOC only.
[c]PM_1 and $PM_{2.5}$ were estimated by this work and the 2011 NEI, respectively.

across different western U.S. ecosystems. For example, compared with the Colockum Tarps fire, the Big Windy Complex and the Rim Fire were in more humid forests with more large trees and surface (e.g., dead wood) and ground fuels (e.g., duff and litter). Thus, the Big Windy Complex and the Rim Fire possibly had higher fuel consumption than the Colockum Tarps fire. However, fuel consumption for western wildfires is not well quantified [*van Leeuwen et al.*, 2014]. Here we averaged the field-measured fuel consumptions of a large wildfire in western Oregon (41.6 Mg ha^{-1} if assuming a carbon fraction of 45.7%) [*Campbell et al.*, 2007] and a prescribed boreal forest fire in Northwest Territories, Canada (27.6 ± 8.7 Mg ha^{-1}) [*Santín et al.*, 2015], which gave 34.6 ± 9.9 Mg ha^{-1}, to represent the average fuel consumption for western wildfires. The components used for emission estimates can all contribute to uncertainty in emission estimates. Quantitative assessments of overall uncertainty in emissions are difficult to make due to limited knowledge about EFs of different fuels and wildfire fuel consumption in different ecosystems. We estimated the emission uncertainty by combining the variations in our EFs and in the two fuel consumption measurements. As mentioned before, the airborne EFs for smoldering species are likely underestimated without including RSC emissions. This could cause our central estimates for CO, total NMOC, and PM_1 (dominated by OA) to be conservative.

Table 5 lists the estimated annual emissions of gases and fine particles from the 11 western states between 2011 and 2015. Also listed are the emissions from wildfires and all other sources in these western states reported by the 2011 NEI (version 2) (http://www.epa.gov/air-emissions-inventories/2011-national-emissions-inventory-nei-data), which is the most recent NEI that has detailed technical documentation available. The 2011 NEI estimated wildfire emissions using EFs from the Fire Emissions Prediction Simulator (FEPS) v2 that relies on EFs from the literature apportioned by flaming and smoldering combustion, fire activity data from multiple sources based on surveys and remote sensing, fuel loading from the Fuel Characteristic Classification System, and fuel consumed estimated by the CONSUME model. The 2011 NEI also states that they have compared area burned by state to the NIFC data to ensure that the values are within a reasonable range. The NIFC burned area in 2011 in these western states is 1,646,695 ha, which is very close to (6.6% less than) the NEI wildfire area (1,762,654 ha). Note that the NIFC 5 year average (1,698,115 ha) is also similar to the 2011 NEI burned area (Table 5). Since uncertainties associated with the NEI estimates are not available, the following comparisons are solely based on the NIFC 5 year average and the NEI values.

Given similar areas burned, the 5 year averaged gas emissions using our EFs show considerable consistency with the 2011 NEI estimates, especially for CO (Table 5). Our estimated flux of CO from wildfires is 5240 ± 2240 Gg yr^{-1} and accounts for ~40% of emissions from all other sources. The total NMOC estimates were based on the EFs measured for the two SEAC^{4}RS fires, which had a more complete suite of NMOC measurements as compared to BBOP. In view of the fact that some important but unmeasured NMOCs (such as acetic acid) were not incorporated into our estimate, the annual emission of 905 ± 437 Gg is likely to be a lower limit. NO_x and SO_2 emissions from western wildfires are 44 ± 41 and 19 ± 22 Gg yr^{-1}, respectively, and are both smaller than the NEI estimates, although not statistically different. The wildfire emissions of NMOC, NO_x, and SO_2 are on the order of a few percent of the total emissions from all other sources.

On the other hand, the western wildfires significantly contribute to the emission of fine particles. Our PM_1 emission of 1530 ± 570 Gg yr^{-1} is over 3 times the NEI $PM_{2.5}$ estimate and almost twice the $PM_{2.5}$ emitted from all other sources. We investigated the possible reason causing our much higher fine PM estimate. As

mentioned before, the burned areas used in this work and by the 2011 NEI are close. In addition, the NEI-used EF(CO) given by the FEPS user's guide is ~107 g kg^{-1} at our average combustion efficiency (~0.87) [*Anderson et al*., 2004], which is ~20% larger than our average EF(CO) of 89.3 ± 28.5 g kg^{-1}. Given similar burned areas, EF(CO)s, and total CO estimates, we would presume that our fuel consumption term should also be similar to that of the NEI, despite our simplified assumptions. Thus, it is likely that our high fine PM emission is due to a higher EF than the values used by the NEI. This is also supported by the FEPS user's guide [*Anderson et al*., 2004], in which EF($PM_{2.5}$) is only ~9 g kg^{-1} at our average combustion efficiency, according to the provided empirical equation of EF as a function of combustion efficiency, as opposed to our average EF(PM_1) of 26.0 ± 6.2 g kg^{-1}. The application of FEPS determined values to the NEI estimates was also confirmed by a U.S. Environmental Protection Agency official.

The magnitude of PM_1 emitted by western U.S. wildfires indicate that a significant fraction of ambient aerosol loading has a BB component, which has important implications for the management of regional air quality. If the EF(PM_1) measured here is a common value for temperate wildfires, the BB-influenced fraction may have been underestimated previously. For example, BB aerosol is difficult to identify after aging due to the decay of marker species such as levoglucosan [*Cubison et al*., 2011]. As OA constitutes the majority of aerosol mass, a better understanding of wildfire impacts downwind requires future emission estimates to account for gas-particle partitioning and photochemical processing of POA emissions.

4. Conclusions

This study significantly updates and expands the range of species measured from temperate wildfires. We present EFs of over 80 trace gases and 5 fine particle components, which will improve emission estimates and the modeling of smoke chemistry and air quality impacts. The EFs of multifunctional organic nitrates and a few OVOCs that are important products from isoprene oxidation were measured for the first time from BB plumes. We also compared our EFs with those from the limited airborne measurements of temperate wildfires, boreal forest fires, and temperate prescribed fires. Among the commonly measured species, most of the NMOC EFs were comparable to the other forest fires listed in Table 3, while the discrepancies in some other NMOCs and sulfur-, nitrogen-, and chlorine-containing gases may be explained by fire variability, chemical and physical properties of fuels, combustion conditions, and photochemical aging. This work also suggests that the aircraft-measured EF(PM_1) from wildfires is substantially larger than that from prescribed fires, which may reflect different fire behavior and fuel conditions between prescribed fires and wildfires. The EFs as a function of MCE were also examined by including data from previous boreal forest fire and prescribed fire studies in North America. The linear fit for EF versus MCE showed good correlation (or anti-correlation) and slopes significantly different from 0 for NO_x, CH_4, several NMOCs, and OA. The EFs of other gases and inorganic PM_1 components are less dependent on MCE and probably more influenced by fuel characteristics and fire variability.

The annual emissions of CO, NO_x, SO_2, total NMOC, and PM_1 from western wildfires in the U.S. were estimated using the observed EFs. The estimated gas emissions are generally comparable with the 2011 NEI. However, due to the high EF(PM_1) measured in this study, our regional PM_1 emissions are over 3 times larger than the NEI $PM_{2.5}$ estimate and almost 2 times larger than the NEI $PM_{2.5}$ emitted from all other sources.

The findings of the large PM EFs and annual emissions from western U.S. wildfires suggest that the current attributions of the percentage of aerosol mass from BB sources may have been significantly underestimated. In addition, these findings could better inform fire management and support the practice of prescribed burning to reduce the impact of PM on air quality. A definitive assessment of the trade-offs between wildfires and prescribed fires will also require confirmation that wildfire events can be reduced significantly by prescribed burning.

Acknowledgments
This work was supported by NASA grants NNX12AB77G, NNX15AT90G, NNX12AC06G, and NNX14AP46G-ACCDAM. The BBOP project was funded by U.S. Department of Energy (DOE) Atmospheric Radiation Measurement (ARM) program and the Atmospheric System Research (ASR) program. P.C.J., D.A.D., B.B.P., and J.L.J. were supported by NASA NNX12AC03G and NNX15AT96G. M. Müller received additional support by the Austrian Space Applications Programme (ASAP 8 and 9, grants 833451 and 840086). ASAP is sponsored by the Austrian Ministry for Transport, Innovation and Technology (BMVIT) and administered by the Aeronautics and Space Agency (ALR) of the Austrian Research Promotion Agency (FFG). The authors would also like to thank the DC-8 and G-1 flight crews. Data from the BBOP and the SEAC^{4}RS missions can be found at http://www.arm.gov/campaigns/bbop and http://www-air.larc.nasa.gov/cgi-bin/ArcView/seac4rs (doi: 10.5067/Aircraft/SEAC4RS/Aerosol-TraceGas-Cloud), respectively. The data generated from this study are available from the authors upon request (greg.huey@eas.gatech.edu).

References

Akagi, S. K., R. J. Yokelson, C. Wiedinmyer, M. J. Alvarado, J. S. Reid, T. Karl, J. D. Crounse, and P. O. Wennberg (2011), Emission factors for open and domestic biomass burning for use in atmospheric models, *Atmos. Chem. Phys.*, *11*(9), 4039–4072, doi:10.5194/acp-11-4039-2011.

Akagi, S. K., et al. (2013), Measurements of reactive trace gases and variable O_3 formation rates in some South Carolina biomass burning plumes, *Atmos. Chem. Phys.*, *13*(3), 1141–1165, doi:10.5194/acp-13-1141-2013.

Alvarado, M. J., et al. (2010), Nitrogen oxides and PAN in plumes from boreal fires during ARCTAS-B and their impact on ozone: An integrated analysis of aircraft and satellite observations, *Atmos. Chem. Phys.*, *10*(20), 9739–9760, doi:10.5194/acp-10-9739-2010.

Anderson, G. K., D. V. Sandberg, and R. A. Norheim (2004) *Fire Emission Production Simulator (FEPS) User's Guide Version 1.0*, Pacific Northwest Research Station, the USDA Forest Service, Seattle, Wash.

Andreae, M. O., and P. Merlet (2001), Emission of trace gases and aerosols from biomass burning, *Global Biogeochem. Cycles*, *15*(4), 955–966, doi:10.1029/2000GB001382.

Bahreini, R., et al. (2009), Organic aerosol formation in urban and industrial plumes near Houston and Dallas, Texas, *J. Geophys. Res.*, *114*, D00F16, doi:10.1029/2008JD011493.

Bates, K. H., T. B. Nguyen, A. P. Teng, J. D. Crounse, H. G. Kjaergaard, B. M. Stoltz, J. H. Seinfeld, and P. O. Wennberg (2016), Production and fate of C_4 dihydroxycarbonyl compounds from isoprene oxidation, *J. Phys. Chem. A*, *120*(1), 106–117, doi:10.1021/acs.jpca.5b10335.

Belsky, A. J., and D. M. Blumenthal (1997), Effects of livestock grazing on stand dynamics and soils in upland forests of the interior west, *Conserv. Biol.*, *11*(2), 315–327, doi:10.1046/j.1523-1739.1997.95405.x.

Bertschi, I. T., R. J. Yokelson, D. E. Ward, R. E. Babbitt, R. A. Susott, J. G. Goode, and W. M. Hao (2003a), Trace gas and particle emissions from fires in large diameter and belowground biomass fuels, *J. Geophys. Res.*, *108*(D13), 8472, doi:10.1029/2002JD002100.

Bertschi, I. T., R. J. Yokelson, D. E. Ward, T. J. Christian, and W. M. Hao (2003b), Trace gas emissions from the production and use of domestic biofuels in Zambia measured by open-path Fourier transform infrared spectroscopy, *J. Geophys. Res.*, *108*(D13), 8469, doi:10.1029/2002JD002158.

Biswell, H. (1999) *Prescribed Burning in California Wildlands Vegetation Management*, Univ. of California Press, Berkeley, Calif.

Brey, S. J., and E. V. Fischer (2016), Smoke in the city: How often and where does smoke impact summertime ozone in the United States?, *Environ. Sci. Technol.*, *50*(3), 1288–1294, doi:10.1021/acs.est.5b05218.

Burling, I. R., et al. (2010), Laboratory measurements of trace gas emissions from biomass burning of fuel types from the southeastern and southwestern United States, *Atmos. Chem. Phys.*, *10*(22), 11115–11130, doi:10.5194/acp-10-11115-2010.

Burling, I. R., R. J. Yokelson, S. K. Akagi, S. P. Urbanski, C. E. Wold, D. W. T. Griffith, T. J. Johnson, J. Reardon, and D. R. Weise (2011), Airborne and ground-based measurements of the trace gases and particles emitted by prescribed fires in the United States, *Atmos. Chem. Phys.*, *11*(23), 12197–12216, doi:10.5194/acp-11-12197-2011.

Campbell, J., D. Donato, D. Azuma, and B. Law (2007), Pyrogenic carbon emission from a large wildfire in Oregon, United States, *J. Geophys. Res.*, *112*, G04014, doi:10.1029/2007JG000451.

Capes, G., B. Johnson, G. McFiggans, P. I. Williams, J. Haywood, and H. Coe (2008), Aging of biomass burning aerosols over West Africa: Aircraft measurements of chemical composition, microphysical properties, and emission ratios, *J. Geophys. Res.*, *113*, *D00C15*, doi:10.1029/2008JD009845.

Christian, T. J., B. Kleiss, R. J. Yokelson, R. Holzinger, P. J. Crutzen, W. M. Hao, B. H. Saharjo, and D. E. Ward (2003), Comprehensive laboratory measurements of biomass-burning emissions: 1. Emissions from Indonesian, African, and other fuels, *J. Geophys. Res.*, *108*(D23), 4719, doi:10.1029/2003JD003704.

Coggon, M. M., et al. (2016), Emissions of nitrogen-containing organic compounds from the burning of herbaceous and arboraceous biomass: Fuel composition dependence and the variability of commonly used nitrile tracers, *Geophys. Res. Lett.*, *43*, 9903–9912, doi:10.1002/2016GL070562.

Collier, S., et al. (2016), Regional influence of aerosol emissions from wildfires driven by combustion efficiency: Insights from the BBOP campaign, *Environ. Sci. Technol.*, *50*(16), 8613–8622, doi:10.1021/acs.est.6b01617.

Crosson, E. R. (2008), A cavity ring-down analyzer for measuring atmospheric levels of methane, carbon dioxide, and water vapor, *Appl. Phys. B: Lasers Opt.*, *92*(3), 403–408, doi:10.1007/s00340-008-3135-y.

Crounse, J. D., K. A. McKinney, A. J. Kwan, and P. O. Wennberg (2006), Measurement of gas-phase hydroperoxides by chemical ionization mass spectrometry, *Anal. Chem.*, *78*(19), 6726–6732, doi:10.1021/ac0604235.

Crounse, J. D., et al. (2009), Biomass burning and urban air pollution over the central Mexican plateau, *Atmos. Chem. Phys.*, *9*(14), 4929–4944, doi:10.5194/acp-9-4929-2009.

Crounse, J. D., F. Paulot, H. G. Kjaergaard, and P. O. Wennberg (2011), Peroxy radical isomerization in the oxidation of isoprene, *Phys. Chem. Chem. Phys.*, *13*(30), 13607–13613, doi:10.1039/C1CP21330J.

Crounse, J. D., L. B. Nielsen, S. Jørgensen, H. G. Kjaergaard, and P. O. Wennberg (2013), Autoxidation of organic compounds in the atmosphere, *J. Phys. Chem. Lett.*, *4*(20), 3513–3520, doi:10.1021/jz4019207.

Crutzen, P. J., and M. O. Andreae (1990), Biomass burning in the tropics: Impact on atmospheric chemistry and biogeochemical cycles, *Science*, *250*(4988), 1669–1678, doi:10.1126/science.250.4988.1669.

Cubison, M. J., et al. (2011), Effects of aging on organic aerosol from open biomass burning smoke in aircraft and laboratory studies, *Atmos. Chem. Phys.*, *11*(23), 12049–12064, doi:10.5194/acp-11-12049-2011.

de Gouw, J. A., C. Warneke, D. D. Parrish, J. S. Holloway, M. Trainer, and F. C. Fehsenfeld (2003), Emission sources and ocean uptake of acetonitrile (CH_3CN) in the atmosphere, *J. Geophys. Res.*, *108*(D11), 4329, doi:10.1029/2002JD002897.

Delfino, R. J., et al. (2009), The relationship of respiratory and cardiovascular hospital admissions to the southern California wildfires of 2003, *Occup. Environ. Med.*, *66*(3), 189–197.

Donaldson, K., L. Tran, L. A. Jimenez, R. Duffin, D. E. Newby, N. Mills, W. MacNee, and V. Stone (2005), Combustion-derived nanoparticles: A review of their toxicology following inhalation exposure, *Part. Fibre Toxicol.*, *2*(1), 1–14, doi:10.1186/1743-8977-2-10.

Fang, T., et al. (2016), Oxidative potential of ambient water-soluble $PM_{2.5}$ in the southeastern United States: Contrasts in sources and health associations between ascorbic acid (AA) and dithiothreitol (DTT) assays, *Atmos. Chem. Phys.*, *16*(6), 3865–3879, doi:10.5194/acp-16-3865-2016.

Forrister, H., et al. (2015), Evolution of brown carbon in wildfire plumes, *Geophys. Res. Lett.*, *42*, 4623–4630, doi:10.1002/2015GL063897.

Friedli, H. R., E. Atlas, V. R. Stroud, L. Giovanni, T. Campos, and L. F. Radke (2001), Volatile organic trace gases emitted from North American wildfires, *Global Biogeochem. Cycles*, *15*(2), 435–452, doi:10.1029/2000GB001328.

Fuentes, J. D., et al. (2000), Biogenic hydrocarbons in the atmospheric boundary layer: A review, *Bull. Am. Meteorol. Soc.*, *81*(7), 1537–1575, doi:10.1175/1520-0477(2000)081<1537:BHITAB>2.3.CO;2.

Goode, J. G., R. J. Yokelson, D. E. Ward, R. A. Susott, R. E. Babbitt, M. A. Davies, and W. M. Hao (2000), Measurements of excess O_3, CO_2, CO, CH_4, C_2H_4, C_2H_2, HCN, NO, NH_3, HCOOH, CH_3COOH, HCHO, and CH_3OH in 1997 Alaskan biomass burning plumes by airborne Fourier transform infrared spectroscopy (AFTIR), *J. Geophys. Res.*, *105*(D17), 22147–22166, doi:10.1029/2000JD900287.

Hardy, C. C., R. D. Ottmar, J. L. Peterson, J. E. Core, and P. Seamon (2001) *Smoke Management Guide for Prescribed and Wildland Fire: 2001 Edition*, National Wildfire Coordination Group, Boise.

Hegg, D. A., L. F. Radke, P. V. Hobbs, R. A. Rasmussen, and P. J. Riggan (1990), Emissions of some trace gases from biomass fires, *J. Geophys. Res.*, *95*(D5), 5669–5675, doi:10.1029/JD095iD05p05669.

Hobbs, P. V., P. Sinha, R. J. Yokelson, T. J. Christian, D. R. Blake, S. Gao, T. W. Kirchstetter, T. Novakov, and P. Pilewskie (2003), Evolution of gases and particles from a savanna fire in South Africa, *J. Geophys. Res.*, *108*(D13), 8485, doi:10.1029/2002JD002352.

Hosseini, S., et al. (2013), Laboratory characterization of PM emissions from combustion of wildland biomass fuels, *J. Geophys. Res. Atmos.*, *118*, 9914–9929, doi:10.1002/jgrd.50481.

Jaffe, D., D. Chand, W. Hafner, A. Westerling, and D. Spracklen (2008), Influence of fires on O_3 concentrations in the western U.S, *Environ. Sci. Technol.*, *42*(16), 5885–5891, doi:10.1021/es800084k.

Jaffe, D. A., and N. L. Wigder (2012), Ozone production from wildfires: A critical review, *Atmos. Environ.*, *51*, 1–10, doi:10.1016/j.atmosenv.2011.11.063.

Jolleys, M. D., et al. (2012), Characterizing the aging of biomass burning organic aerosol by use of mixing ratios: A meta-analysis of four regions, *Environ. Sci. Technol.*, *46*(24), 13093–13102, doi:10.1021/es302386v.

Jolleys, M. D., et al. (2015), Properties and evolution of biomass burning organic aerosol from Canadian boreal forest fires, *Atmos. Chem. Phys.*, *15*(6), 3077–3095, doi:10.5194/acp-15-3077-2015.

Kilgore, B. M. (1981), Fire in ecosystem distribution and structure : Western forests and scrublands, in *Proceedings of the Conference: Fire Regimes and Ecosystem Properties*, edited by H. A. Mooney, T. M. Bonnicksen and N. L. Christensen, pp. 58–89, USDA Forest Service, General Technical Report WO-GTR-26.

Künzli, N., et al. (2006), Health effects of the 2003 Southern California wildfires on children, *Am. J. Respir. Crit. Care Med.*, *174*(11), 1221–1228, doi:10.1164/rccm.200604-519OC.

Lee, A. K. Y., M. D. Willis, R. M. Healy, T. B. Onasch, and J. P. D. Abbatt (2015), Mixing state of carbonaceous aerosol in an urban environment: Single particle characterization using the soot particle aerosol mass spectrometer (SP-AMS), *Atmos. Chem. Phys.*, *15*(4), 1823–1841, doi:10.5194/acp-15-1823-2015.

Lee, B. H., et al. (2016), Highly functionalized organic nitrates in the southeast United States: Contribution to secondary organic aerosol and reactive nitrogen budgets, *Proc. Natl. Acad. Sci. U.S.A.*, *113*(6), 1516–1521.

Lee, L., A. P. Teng, P. O. Wennberg, J. D. Crounse, and R. C. Cohen (2014), On rates and mechanisms of OH and O_3 reactions with isoprene-derived hydroxy nitrates, *J. Phys. Chem. A*, *118*(9), 1622–1637, doi:10.1021/jp4107603.

Lelieveld, J., et al. (2008), Atmospheric oxidation capacity sustained by a tropical forest, *Nature*, *452*(7188), 737–740, doi:10.1038/nature06870.

Lewis, K. A., et al. (2009), Reduction in biomass burning aerosol light absorption upon humidification: Roles of inorganically-induced hygroscopicity, particle collapse, and photoacoustic heat and mass transfer, *Atmos. Chem. Phys.*, *9*(22), 8949–8966, doi:10.5194/acp-9-8949-2009.

Li, Q., D. J. Jacob, I. Bey, R. M. Yantosca, Y. Zhao, Y. Kondo, and J. Notholt (2000), Atmospheric hydrogen cyanide (HCN): Biomass burning source, ocean sink?, *Geophys. Res. Lett.*, *27*(3), 357–360, doi:10.1029/1999GL010935.

Lindinger, W., A. Hansel, and A. Jordan (1998), On-line monitoring of volatile organic compounds at pptv levels by means of proton-transfer-reaction mass spectrometry (PTR-MS) medical applications, food control and environmental research, *Int. J. Mass Spectrom. Ion Processes*, *173*(3), 191–241, doi:10.1016/S0168-1176(97)00281-4.

Liu, X., et al. (2016), Agricultural fires in the southeastern U.S. during SEAC^{4}RS: Emissions of trace gases and particles and evolution of ozone, reactive nitrogen, and organic aerosol, *J. Geophys. Res. Atmos.*, *121*, 7383–7414, doi:10.1002/2016JD025040.

Lobert, J. M., D. H. Scharffe, W. M. Hao, T. A. Kuhlbusch, R. Seuwen, P. Warneck, and P. J. Crutzen (1991), Experimental evaluation of biomass burning emissions: Nitrogen and carbon containing compounds, in *Global Biomass Burning: Atmospheric, Climatic, and Biospheric Implications*, edited by J. S. Levine, pp. 289–304, MIT Press, Cambridge, Mass.

Lobert, J. M., W. C. Keene, J. A. Logan, and R. Yevich (1999), Global chlorine emissions from biomass burning: Reactive chlorine emissions inventory, *J. Geophys. Res.*, *104*(D7), 8373, doi:10.1029/1998JD100077.

Marlon, J. R., et al. (2012), Long-term perspective on wildfires in the western USA, *Proc. Natl. Acad. Sci. U.S.A.*, *109*(9), E535–E543.

May, A. A., et al. (2014), Aerosol emissions from prescribed fires in the United States: A synthesis of laboratory and aircraft measurements, *J. Geophys. Res. Atmos.*, *119*, 11,826–11,849, doi:10.1002/2014JD021848.

McKenzie, L. M., D. E. Ward, and W. M. Hao (1996), Chlorine and bromine in the biomass of tropical and temperate ecosystems, in *Biomass Burning and Global Change*, edited by J. S. Levin, pp. 241–248, MIT Press, Cambridge, Mass.

McMeeking, G. R., et al. (2009), Emissions of trace gases and aerosols during the open combustion of biomass in the laboratory, *J. Geophys. Res.*, *114*, D19210, doi:10.1029/2009JD011836.

Müller, M., et al. (2016), In situ measurements and modeling of reactive trace gases in a small biomass burning plume, *Atmos. Chem. Phys.*, *16*(6), 3813–3824, doi:10.5194/acp-16-3813-2016.

Naeher, L. P., M. Brauer, M. Lipsett, J. T. Zelikoff, C. D. Simpson, J. Q. Koenig, and K. R. Smith (2007), Woodsmoke health effects: A review, *Inhalation Toxicol.*, *19*(1), 67–106, doi:10.1080/08958370600985875.

Onasch, T. B., A. Trimborn, E. C. Fortner, J. T. Jayne, G. L. Kok, L. R. Williams, P. Davidovits, and D. R. Worsnop (2012), Soot particle aerosol mass spectrometer: Development, validation, and initial application, *Aerosol Sci. Technol.*, *46*(7), 804–817, doi:10.1080/02786826.2012.663948.

Park, R. J., D. J. Jacob, and J. A. Logan (2007), Fire and biofuel contributions to annual mean aerosol mass concentrations in the United States, *Atmos. Environ.*, *41*(35), 7389–7400, doi:10.1016/j.atmosenv.2007.05.061.

Paulot, F., J. D. Crounse, H. G. Kjaergaard, J. H. Kroll, J. H. Seinfeld, and P. O. Wennberg (2009a), Isoprene photooxidation: New insights into the production of acids and organic nitrates, *Atmos. Chem. Phys.*, *9*(4), 1479–1501, doi:10.5194/acp-9-1479-2009.

Paulot, F., J. D. Crounse, H. G. Kjaergaard, A. Kurten, J. M. S. Clair, J. H. Seinfeld, and P. O. Wennberg (2009b), Unexpected epoxide formation in the gas-phase photooxidation of isoprene, *Science*, *325*(5941), 730–733, doi:10.1126/science.1172910.

Perring, A. E., S. E. Pusede, and R. C. Cohen (2013), An observational perspective on the atmospheric impacts of alkyl and multifunctional nitrates on ozone and secondary organic aerosol, *Chem. Rev.*, *113*(8), 5848–5870, doi:10.1021/cr300520x.

Peterson, D. A., E. J. Hyer, J. R. Campbell, M. D. Fromm, J. W. Hair, C. F. Butler, and M. A. Fenn (2014), The 2013 Rim Fire: Implications for predicting extreme fire spread, pyroconvection, and smoke emissions, *Bull. Am. Meteorol. Soc.*, *96*(2), 229–247, doi:10.1175/BAMS-D-14-00060.1.

Radke, L. F., D. A. Hegg, P. V. Hobbs, J. D. Nance, J. H. Lyons, K. K. Laursen, R. E. Weiss, P. J. Riggan, and D. E. Ward (1991), Particulate and trace gas emissions from large biomass fire in North America, in *Global Biomass Burning: Atmospheric, Climatic, and Biospheric Implications*, edited by J. S. Levine, pp. 209–224, MIT Press, Cambridge, Mass.

Reid, J. S., R. Koppmann, T. F. Eck, and D. P. Eleuterio (2005), A review of biomass burning emissions part II: Intensive physical properties of biomass burning particles, *Atmos. Chem. Phys.*, *5*(3), 799–825, doi:10.5194/acp-5-799-2005.

Reinhardt, T. E., and D. E. Ward (1995), Factors affecting methyl chloride emissions from forest biomass combustion, *Environ. Sci. Technol.*, *29*(3), 825–832, doi:10.1021/es00003a034.
Rudolph, J., A. Khedim, R. Koppmann, and B. Bonsang (1995), Field study of the emissions of methyl chloride and other halocarbons from biomass burning in western Africa, *J. Atmos. Chem.*, *22*(1), 67–80, doi:10.1007/BF00708182.
Saleh, R., C. J. Hennigan, G. R. McMeeking, W. K. Chuang, E. S. Robinson, H. Coe, N. M. Donahue, and A. L. Robinson (2013), Absorptivity of brown carbon in fresh and photo-chemically aged biomass-burning emissions, *Atmos. Chem. Phys.*, *13*(15), 7683–7693, doi:10.5194/acp-13-7683-2013.
Santín, C., S. H. Doerr, C. M. Preston, and G. González-Rodríguez (2015), Pyrogenic organic matter production from wildfires: A missing sink in the global carbon cycle, *Global Change Biol.*, *21*(4), 1621–1633, doi:10.1111/gcb.12800.
Savage, M., and T. W. Swetnam (1990), Early 19th-century fire decline following sheep pasturing in a Navajo ponderosa pine forest, *Ecology*, *71*(6), 2374–2378, doi:10.2307/1938649.
Seiler, W., and P. Crutzen (1980), Estimates of gross and net fluxes of carbon between the biosphere and the atmosphere from biomass burning, *Clim. Change*, *2*(3), 207–247, doi:10.1007/BF00137988.
Shilling, J. E., et al. (2013), Enhanced SOA formation from mixed anthropogenic and biogenic emissions during the CARES campaign, *Atmos. Chem. Phys.*, *13*(4), 2091–2113, doi:10.5194/acp-13-2091-2013.
Simmonds, P. G., et al. (2006), Global trends, seasonal cycles, and European emissions of dichloromethane, trichloroethene, and tetrachloroethene from the AGAGE observations at Mace Head, Ireland, and Cape Grim, Tasmania, *J. Geophys. Res.*, *111*, D18304, doi:10.1029/2006JD007082.
Simpson, I. J., et al. (2011), Boreal forest fire emissions in fresh Canadian smoke plumes: C_1–C_{10} volatile organic compounds (VOCs), CO_2, CO, NO_2, NO, HCN and CH_3CN, *Atmos. Chem. Phys.*, *11*(13), 6445–6463, doi:10.5194/acp-11-6445-2011.
Singh, H. B., et al. (2010), Pollution influences on atmospheric composition and chemistry at high northern latitudes: Boreal and California forest fire emissions, *Atmos. Environ.*, *44*(36), 4553–4564, doi:10.1016/j.atmosenv.2010.08.026.
Singh, H. B., C. Cai, A. Kaduwela, A. Weinheimer, and A. Wisthaler (2012), Interactions of fire emissions and urban pollution over California: Ozone formation and air quality simulations, *Atmos. Environ.*, *56*, 45–51, doi:10.1016/j.atmosenv.2012.03.046.
St. Clair, J. M., K. M. Spencer, M. R. Beaver, J. D. Crounse, F. Paulot, and P. O. Wennberg (2014), Quantification of hydroxyacetone and glycolaldehyde using chemical ionization mass spectrometry, *Atmos. Chem. Phys.*, *14*(8), 4251–4262, doi:10.5194/acp-14-4251-2014.
Stevens, J. T., H. D. Safford, and A. M. Latimer (2014), Wildfire-contingent effects of fuel treatments can promote ecological resilience in seasonally dry conifer forests, *Can. J. For. Res.*, *44*(8), 843–854, doi:10.1139/cjfr-2013-0460.
Stockwell, C. E., R. J. Yokelson, S. M. Kreidenweis, A. L. Robinson, P. J. DeMott, R. C. Sullivan, J. Reardon, K. C. Ryan, D. W. T. Griffith, and L. Stevens (2014), Trace gas emissions from combustion of peat, crop residue, domestic biofuels, grasses, and other fuels: Configuration and Fourier transform infrared (FTIR) component of the fourth Fire Lab at Missoula Experiment (FLAME-4), *Atmos. Chem. Phys.*, *14*(18), 9727–9754, doi:10.5194/acp-14-9727-2014.
Stockwell, C. E., P. R. Veres, J. Williams, and R. J. Yokelson (2015), Characterization of biomass burning emissions from cooking fires, peat, crop residue, and other fuels with high-resolution proton-transfer-reaction time-of-flight mass spectrometry, *Atmos. Chem. Phys.*, *15*(2), 845–865, doi:10.5194/acp-15-845-2015.
Surratt, J. D., A. W. H. Chan, N. C. Eddingsaas, M. Chan, C. L. Loza, A. J. Kwan, S. P. Hersey, R. C. Flagan, P. O. Wennberg, and J. H. Seinfeld (2010), Reactive intermediates revealed in secondary organic aerosol formation from isoprene, *Proc. Natl. Acad. Sci. U.S.A.*, *107*(15), 6640–6645.
Susott, R. A., G. J. Olbu, S. P. Baker, D. E. Ward, J. B. Kauffman, and R. W. Shea (1996), Carbon, hydrogen, nitrogen, and thermogravimetric analysis of tropical ecosystem biomass, in *Biomass Burning and Global Change*, edited by J. S. Levine, pp. 249–259, MIT Press, Cambridge.
Teng, A. P., J. D. Crounse, L. Lee, J. M. S. Clair, R. C. Cohen, and P. O. Wennberg (2015), Hydroxy nitrate production in the OH-initiated oxidation of alkenes, *Atmos. Chem. Phys.*, *15*(8), 4297–4316, doi:10.5194/acp-15-4297-2015.
Toon, O. B., et al. (2016), Planning, implementation and scientific goals of the Studies of Emissions and Atmospheric Composition, Clouds and Climate Coupling by Regional Surveys ($SEAC^4RS$) field mission, *J. Geophys. Res. Atmos.*, *121*, 4967–5009, doi:10.1002/2015JD024297.
Turetsky, M. R., E. S. Kane, J. W. Harden, R. D. Ottmar, K. L. Manies, E. Hoy, and E. S. Kasischke (2011), Recent acceleration of biomass burning and carbon losses in Alaskan forests and peatlands, *Nat. Geosci.*, *4*(1), 27–31, doi:10.1038/ngeo1027.
Urbanski, S. P. (2013), Combustion efficiency and emission factors for wildfire-season fires in mixed conifer forests of the northern Rocky Mountains, US, *Atmos. Chem. Phys.*, *13*(14), 7241–7262, doi:10.5194/acp-13-7241-2013.
van Leeuwen, T. T., et al. (2014), Biomass burning fuel consumption rates: A field measurement database, *Biogeosciences*, *11*(24), 7305–7329, doi:10.5194/bg-11-7305-2014.
Verma, V., T. Fang, H. Guo, L. King, J. T. Bates, R. E. Peltier, E. Edgerton, A. G. Russell, and R. J. Weber (2014), Reactive oxygen species associated with water-soluble $PM_{2.5}$ in the southeastern United States: Spatiotemporal trends and source apportionment, *Atmos. Chem. Phys.*, *14*(23), 12,915–12,930, doi:10.5194/acp-14-12915-2014.
Washenfelder, R. A., et al. (2015), Biomass burning dominates brown carbon absorption in the rural southeastern United States, *Geophys. Res. Lett.*, *42*, 653–664, doi:10.1002/2014gl062444.
Westerling, A. L., H. G. Hidalgo, D. R. Cayan, and T. W. Swetnam (2006), Warming and earlier spring increase western U.S. forest wildfire activity, *Science*, *313*(5789), 940–943.
Yang, A., N. A. H. Janssen, B. Brunekreef, F. R. Cassee, G. Hoek, and U. Gehring (2016), Children's respiratory health and oxidative potential of $PM_{2.5}$: The PIAMA birth cohort study, *Occup. Environ. Med.*, *73*(3), 154–160.
Yates, E. L., et al. (2016), Airborne measurements and emission estimates of greenhouse gases and other trace constituents from the 2013 California Yosemite Rim wildfire, *Atmos. Environ.*, *127*, 293–302, doi:10.1016/j.atmosenv.2015.12.038.
Yokelson, R. J., D. W. T. Griffith, and D. E. Ward (1996), Open-path Fourier transform infrared studies of large-scale laboratory biomass fires, *J. Geophys. Res.*, *101*(D15), 21067, doi:10.1029/96JD01800.
Yokelson, R. J., R. Susott, D. E. Ward, J. Reardon, and D. W. T. Griffith (1997), Emissions from smoldering combustion of biomass measured by open-path Fourier transform infrared spectroscopy, *J. Geophys. Res.*, *102*(D15), 18865, doi:10.1029/97JD00852.
Yokelson, R. J., J. G. Goode, D. E. Ward, R. A. Susott, R. E. Babbitt, D. D. Wade, I. Bertschi, D. W. T. Griffith, and W. M. Hao (1999), Emissions of formaldehyde, acetic acid, methanol, and other trace gases from biomass fires in North Carolina measured by airborne Fourier transform infrared spectroscopy, *J. Geophys. Res.*, *104*(D23), 30109, doi:10.1029/1999JD900817.
Yokelson, R. J., T. J. Christian, T. G. Karl, and A. Guenther (2008), The tropical forest and fire emissions experiment: Laboratory fire measurements and synthesis of campaign data, *Atmos. Chem. Phys.*, *8*(13), 3509–3527, doi:10.5194/acp-8-3509-2008.
Yokelson, R. J., et al. (2009), Emissions from biomass burning in the Yucatan, *Atmos. Chem. Phys.*, *9*(15), 5785–5812, doi:10.5194/acp-9-5785-2009.

Yokelson, R. J., I. R. Burling, S. P. Urbanski, E. L. Atlas, K. Adachi, P. R. Buseck, C. Wiedinmyer, S. K. Akagi, D. W. Toohey, and C. E. Wold (2011), Trace gas and particle emissions from open biomass burning in Mexico, *Atmos. Chem. Phys.*, *11*(14), 6787–6808, doi:10.5194/acp-11-6787-2011.

Yokelson, R. J., et al. (2013), Coupling field and laboratory measurements to estimate the emission factors of identified and unidentified trace gases for prescribed fires, *Atmos. Chem. Phys.*, *13*(1), 89–116, doi:10.5194/acp-13-89-2013.